Temperature explains broad patterns of Ross River virus transmission

Marta S. Shocket[1*] (mshocket@stanford.edu), Sadie J. Ryan[2,3,4] (sjryan@ufl.edu), and Erin A. Mordecai[1] (emordeca@stanford.edu)

[1]Department of Biology, Stanford University, 371 Serra Mall, Stanford, CA, USA

[2]Department of Geography, University of Florida, Turlington Hall, Gainesville, FL, USA

[3]Emerging Pathogens Institute, University of Florida, Gainesville, FL, USA

[4]School of Life Sciences, College of Agriculture, Engineering, and Science, University of KwaZulu Natal, Scottsville, KwaZulu Natal, South Africa

Authorship statement: EAM conceived of and designed the study. MSS collected data, performed statistical analyses, and wrote the first draft of the manuscript. SJR performed geographic analyses. All authors revised and approved the manuscript.

Data accessibility statement: Upon acceptance, all data will be archived in Dryad repository.

Competing Interests Statement: We have no competing interests.

Keywords: *Aedes vigilax*, *Culex annulirostris*, mosquito-borne disease, infectious disease, Ross River virus, temperature

* Corresponding Author: Marta S. Shocket, mshocket@stanford.edu, phone: 650-723-5923

ABSTRACT

Thermal biology predicts that vector-borne disease transmission peaks at intermediate temperatures and declines at high and low temperatures. However, thermal optima and limits remain unknown for most vector-borne pathogens. We built a mechanistic model for the thermal response of Ross River virus, an important mosquito-borne pathogen in Australia, Pacific Islands, and potentially emerging worldwide. Transmission peaks at moderate temperatures (26.4°C) and declines to zero at thermal limits (17.0°C and 31.5°C). The model accurately predicts that transmission is year-round endemic in the tropics but seasonal in temperate areas, and matches the nationwide seasonal peak in human cases. Climate warming will likely increase transmission in temperate areas (where most Australians live) but decrease transmission in tropical areas where mean temperatures are already near the thermal optimum. These results illustrate the importance of nonlinear models for inferring the role of temperature in disease dynamics and predicting responses to climate change.

34 **INTRODUCTION**

35 Temperature impacts transmission of mosquito-borne diseases via effects on the
36 physiology of mosquitoes and pathogens. Transmission requires that mosquitoes be abundant,
37 bite a host and ingest an infectious bloodmeal, survive long enough for pathogen development
38 and within-host migration (the extrinsic incubation period), and bite additional hosts—all
39 processes that depend on temperature (Mordecai et al. 2013, 2017). Although both mechanistic
40 (Mordecai et al. 2013, 2017, Liu-Helmersson et al. 2014, Wesolowski et al. 2015, Paull et al.
41 2017) and statistical models (Perkins et al. 2015, Siraj et al. 2015, Paull et al. 2017, Peña-García
42 et al. 2017) support the impact of temperature on mosquito-borne disease, important knowledge
43 gaps remain. First, how the impact of temperature on transmission differs across diseases, via
44 what mechanisms, and the types of data needed to characterize these differences all remain
45 uncertain. Second, the impacts of temperature on transmission can appear idiosyncratic—varying
46 in both magnitude and direction—across locations and studies (Gatton et al. 2005, Stewart Ibarra
47 and Lowe 2013, Peña-García et al. 2017). Although inferring causality from field observations
48 and statistical approaches alone remains challenging, nonlinear thermal biology may
49 mechanistically explain this variation. As the climate changes, filling these gaps becomes
50 increasingly important for predicting geographic, seasonal, and interannual variation in
51 transmission of mosquito-borne pathogens. Here, we address these gaps by building a model for
52 temperature-dependent transmission of Ross River virus (RRV), the most important mosquito-
53 borne disease in Australia (1,500–9,500 human cases per year) (Koolhof et al. 2017), and a
54 potentially emerging pathogen worldwide (Flies et al. 2018).

55 RRV in Australia is an ideal case study for examining the influence of temperature.
56 Transmission occurs across a wide latitudinal gradient, where climate varies substantially both

57 geographically and seasonally. Moreover, compared to vector-borne diseases in lower-income
58 settings, RRV case diagnosis and reporting are accurate and consistent, and variation in
59 socioeconomic conditions (and therefore housing and vector control efforts) at regional and
60 continental scales is relatively low. Previous work has shown that in some settings temperature
61 predicts RRV cases (Gatton et al. 2005, Bi et al. 2009, Werner et al. 2012, Koolhof et al. 2017),
62 while in others it does not (Hu et al. 2004, Gatton et al. 2005). Understanding RRV transmission
63 ecology is critical because the virus is a likely candidate for emergence worldwide (Flies et al.
64 2018), and has caused explosive epidemics where it has emerged in the past (infecting over
65 500,000 people in a 1979-80 epidemic in Fiji) (Klapsing et al. 2005). RRV is a significant public
66 health burden because infection causes joint pain that can become chronic and cause disability
67 (Harley et al. 2001, Koolhof et al. 2017). A mechanistic model for temperature-dependent
68 transmission could help explain these disparate results and predict potential expansion.
69 Mechanistic models synthesize how environmental factors like temperature influence
70 host and parasite traits that drive transmission. Thermal responses of ectotherm traits are usually
71 unimodal: they peak at intermediate temperatures and decline towards zero at lower and upper
72 thermal limits, all of which vary across traits (Dell et al. 2011, Mordecai et al. 2013, 2017).
73 Mechanistic models are particularly useful for synthesizing the effects of multiple, nonlinear
74 thermal responses that shape transmission (Rogers and Randolph 2006, Mordecai et al. 2013).
75 One commonly used measure of disease spread is R_0, the basic reproductive number (secondary
76 cases expected from a single case in a fully susceptible population). For mosquito-borne disease,
77 R_0 is a nonlinear function of mosquito density, biting rate, vector competence (infectiousness
78 given pathogen exposure), and adult survival; pathogen extrinsic incubation period; and human
79 recovery rate (Dietz 1993). To understand how multiple traits that respond nonlinearly to

80 temperature combine to affect transmission, we incorporate empirically-estimated trait thermal
81 responses into an R_0 model. Synthesizing the full suite of nonlinear trait responses is critical
82 because such models often make predictions that are drastically different, with transmission
83 optima up to 7ºC lower, than models that assume linear or monotonic thermal responses or omit
84 temperature-dependent processes (Mordecai et al. 2013, 2017). Previous mechanistic models that
85 incorporate multiple nonlinear trait thermal responses have predicted different optimal
86 temperatures across pathogens and vector species: 25ºC for *falciparum* malaria and West Nile
87 virus (Mordecai et al. 2013, Paull et al. 2017), and 29ºC and 26 ºC for dengue, chikungunya, and
88 Zika viruses in *Ae. aegypti* and *Ae. albopictus*, respectively (Liu-Helmersson et al. 2014,
89 Wesolowski et al. 2015, Mordecai et al. 2017).

90 Here, we build the first mechanistic model for temperature-dependent transmission of
91 RRV and ask whether temperature explains seasonal and geographic patterns of disease. We use
92 data from laboratory experiments with two important and well-studied vector species (*Culex*
93 *annulirostris* and *Aedes vigilax*) to parameterize the model with unimodal thermal responses. We
94 then use sensitivity and uncertainty analyses to determine which traits drive the relationship
95 between temperature and transmission potential and identify key data gaps. Finally, we illustrate
96 how temperature currently shapes patterns of disease transmission across Australia. The model
97 correctly predicts that RRV disease is year-round endemic in tropical, northern Australia with
98 little seasonal variation due to temperature and seasonally epidemic in temperate, southern
99 Australia. These results provides a mechanistic explanation for idiosyncrasies in RRV
100 temperature responses observed in previous studies (Hu et al. 2004, Gatton et al. 2005, Bi et al.
101 2009, Werner et al. 2012, Koolhof et al. 2017). A population-weighted version of the model also
102 accurately predicts the seasonality of human cases nationally. Thus, from laboratory data on

103 mosquito and parasite thermal responses alone, this simple model mechanistically explains broad
104 geographic and seasonal patterns of disease.
105
106 *Natural History of RRV*
107 The natural history of RRV is complex: transmission occurs across a range of climates
108 (tropical, subtropical, and temperate) and habitats (urban and rural, coastal and inland) and via
109 many vector and vertebrate reservoir species (Claflin and Webb 2015). The virus has been
110 isolated from over 40 mosquito species in nature, and 10 species transmit it in laboratory studies
111 (Harley et al. 2001, Russell 2002). However, four species are responsible for most transmission
112 to humans (*Culex annulirostris*, *Aedes [Ochlerotatus] vigilax*, *Ae. [O.] notoscriptus*, and *Ae.*
113 *[O.] camptorhynchus*), with two additional species implicated in outbreaks (*Ae. [Stegomyia]*
114 *polynesiensis* and *Ae. [O.] normanensis*).
115 The vectors differ in climate and habitat niches, leading to geographic variation in
116 associations with outbreaks. We assembled and mapped records of RRV outbreaks in humans
117 attributed to different vector species (Fig. 1, Table S1). *Ae. vigilax* and *Ae. notoscriptus* were
118 more commonly implicated in transmission in tropical and subtropical zones, *Ae.*
119 *camptorhynchus* in temperate zones, and *Cx. annulirostris* throughout all climatic zones.
120 Freshwater-breeding *Cx. annulirostris* has been implicated in transmission across both inland
121 and coastal areas, while saltmarsh mosquitoes *Ae. vigilax* and *Ae. camptorhynchus* have been
122 implicated only in coastal areas (Russell 2002) and inland areas affected by salinization from
123 agriculture (Biggs and Mottram 2008, Carver et al. 2009). Peri-domestic, container-breeding *Ae.*
124 *notoscriptus* has been implicated in urban epidemics (Russell 2002). The vectors also differ in
125 their seasonality: *Ae. camptorhynchus* populations peak earlier and in cooler temperatures than

126 *Ae. vigilax*, leading to seasonal succession where they overlap (Russell 1998). This latitudinal
127 and temporal variation suggests that vector species may have different thermal optima and/or
128 niche breadths. If so, temperature may impact disease transmission differently for each species.

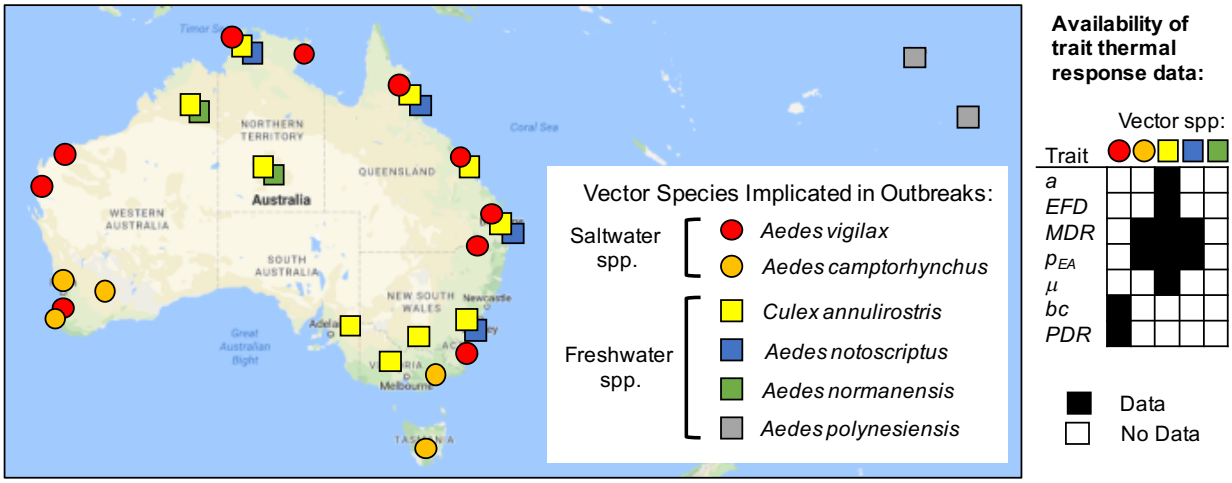

129

130 **FIGURE 1: Vector species implicated in RRV disease outbreaks.** Map of specific mosquito
131 species identified as important vectors based on collected field specimens. Grid (right) shows
132 data availability of trait thermal responses for the five Australian species. Data sources listed in
133 Table S1. Trait parameters defined in Methods.

134

135 *General Modelling Approach*

136 R_0 depends on a suite of vector, pathogen, and human traits, including vector density.
137 Vector density depends on both temperature-dependent traits and aquatic breeding habitat
138 (Barton et al. 2004, Kokkinn et al. 2009, Jacups et al. 2015). Therefore, we developed two R_0
139 models: the 'Constant *M* Model' (eq. 1) assumes mosquito density (*M*) does not depend on
140 temperature (Dietz 1993); the 'Temperature-Dependent *M* Model' (eq. 2) assumes temperature
141 drives mosquito density and includes vector life history trait thermal responses (Parham and
142 Michael 2010, Mordecai et al. 2013, 2017). The relative influence of temperature versus habitat
143 availability and other drivers varies across settings; these models capture two extremes. Because

144 habitat availability is context-dependent and species-specific, and because we focus on
145 temperature, we do not model vector habitat here. We initially compare results for both models,
146 then focus on the temperature-dependent *M* model.

147 Since R_0 also depends on other factors, we scaled model output between zero and one
148 ('relative R_0'). Relative R_0 describes thermal suitability for transmission, which combines with
149 factors like breeding habitat availability, vector control, humidity, human and reservoir host
150 density, host immune status, and mosquito exposure to determine disease incidence. In this
151 approach, only the relative thermal response of each trait influences R_0, desirable since traits can
152 differ substantially due to other factors and in laboratory versus field settings (particularly
153 mosquito survival: Clements and Paterson 1981). For relative R_0 we cannot use the typical
154 threshold for sustained disease transmission (R_0>1). However, relative R_0 preserves the
155 temperature-dependence of R_0, including key temperature values: where transmission is possible
156 (R_0>0; a conservative threshold where transmission is not excluded by temperature) and where
157 R_0 is maximized.

158

159 **RESULTS**

160 Vector and pathogen traits that drive transmission consistently responded to temperature
161 (Fig. 2), though data were sparse (Table S2) (McDonald et al. 1980, Mottram et al. 1986, Russell
162 1986, Rae 1990, Kay and Jennings 2002). Although we exhaustively searched for experiments
163 with trait measurements at three or more constant temperatures in the Australian vector species
164 (*Cx. annulirostris*, *Ae. vigilax*, *Ae. camptorhynchus*, *Ae. notoscriptus*, and *Ae. normanensis*), no
165 species had data for all necessary traits (Fig. 1). Thus, we combined mosquito life history traits
166 from *Cx. annulirostris* and infection traits measured in *Ae. vigilax* to build composite R_0 models.

167 We also fit traits for other mosquito and virus species: *MDR* and *pEA* from *Ae. camptorhynchus*

168 and *Ae. notoscriptus*, and *PDR* and *bc* from Murray Valley encephalitis virus (another important

169 pathogen transmitted by these mosquitoes in Australia) in *Cx. annulirostris* (see Appendix). We

170 use sensitivity analyses to evaluate the potential impact of this vector mismatch.

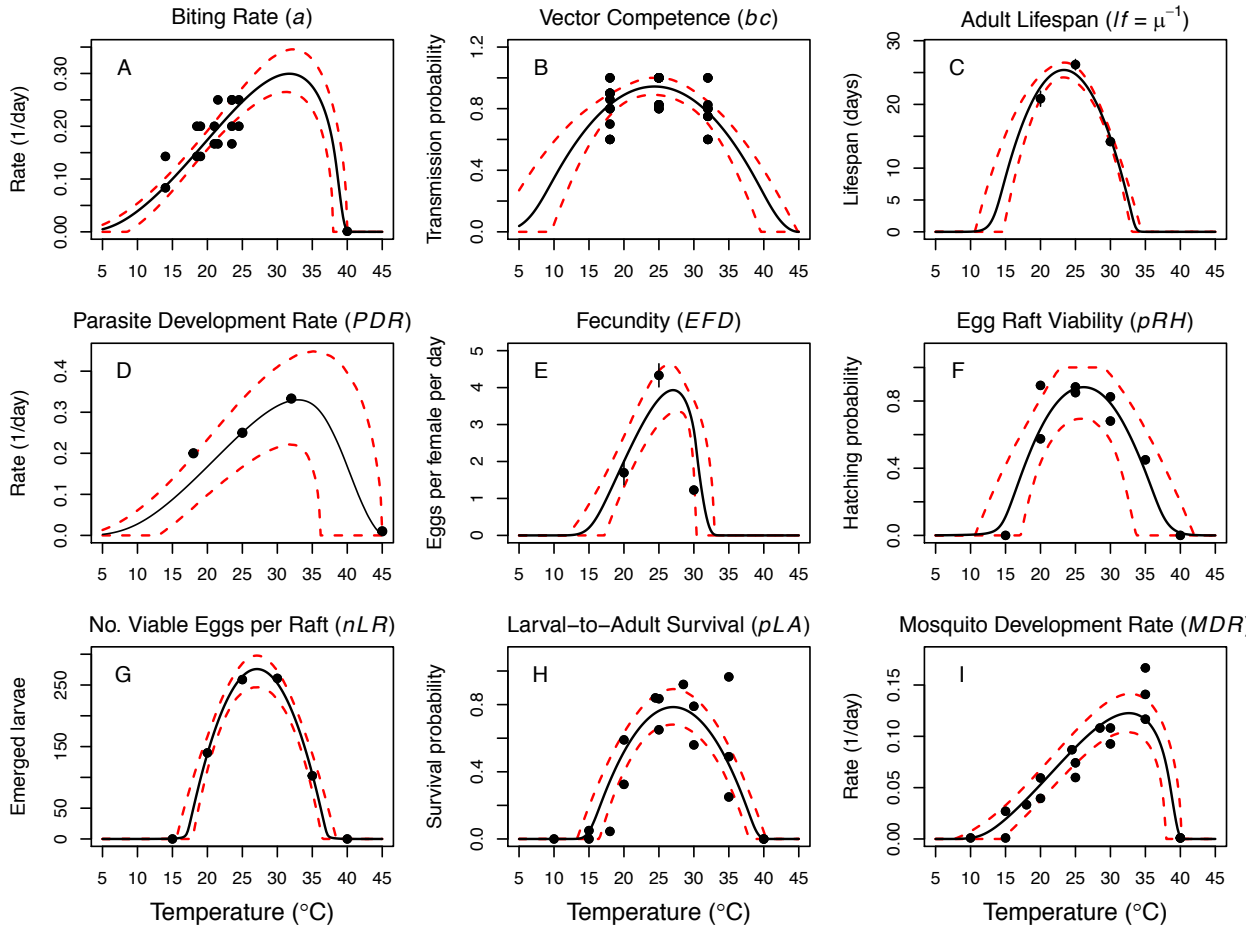

171

172 **FIGURE 2**: **Thermal responses of *Cx. annulirostris* and RRV (in *Ae. vigilax*) traits that**

173 **drive transmission**. Functions were fit using Bayesian inference with priors fit using data from

174 other mosquito species and viruses. Black solid lines are posterior distribution means; dashed red

175 lines are 95% credible intervals. (E, C) Points are data means; error bars are standard error.

176

177 Thermal optima ranged from 23.4ºC for adult lifespan (*lf*) to 33.0ºC for parasite
178 development rate (*PDR*; Fig. 2). The data supported unimodal thermal responses for most traits,
179 though declines at high temperatures were not directly observed for biting rate (*a*) and parasite
180 development rate. Instead, data from other mosquito species and ectotherm physiology theory
181 imply these traits must decline at very high temperatures (~40ºC).
182 The optimal temperature for transmission (relative R_0) peaked near 26.4ºC regardless of
183 whether or not mosquito density [*M*] depended on temperature, because optimal transmission
184 aligned with optimal mosquito density (Fig. 3; temperature-dependent *M* model: 26.4ºC, constant
185 *M* model: 26.6ºC, *M* 26.2ºC). By contrast, the range of temperatures suitable for transmission is
186 much narrower when mosquito density depends on temperature because *M*(*T*) constrains
187 transmission at the thermal limits (Fig. 3; temperature-dependent *M* model: 17.0–31.5ºC,
188 constant *M* model: 12.9–33.7ºC). The thermal constraints that mosquito density imposes on
189 transmission are important because, although demographic traits are well-known to vary with
190 temperature in the laboratory, many temperature-dependent transmission models do not assume
191 that temperature influences mosquito density (Martens et al. 1997, Craig et al. 1999, Caminade et
192 al. 2017, Paull et al. 2017, Hamlet et al. 2018, but see Parham and Michael 2010, Mordecai et al.
193 2013, 2017, Johnson et al. 2015). The moderate optimal temperature for RRV (26-27ºC) fits
194 within the range of thermal optima found for other diseases: malaria transmission by *Anopheles*
195 spp. at 25ºC, and dengue and other viruses by *Ae. aegypti* and *Ae. albopictus* at 29ºC and 26ºC,
196 respectively (Fig. 4) (Mordecai et al. 2013, 2017).

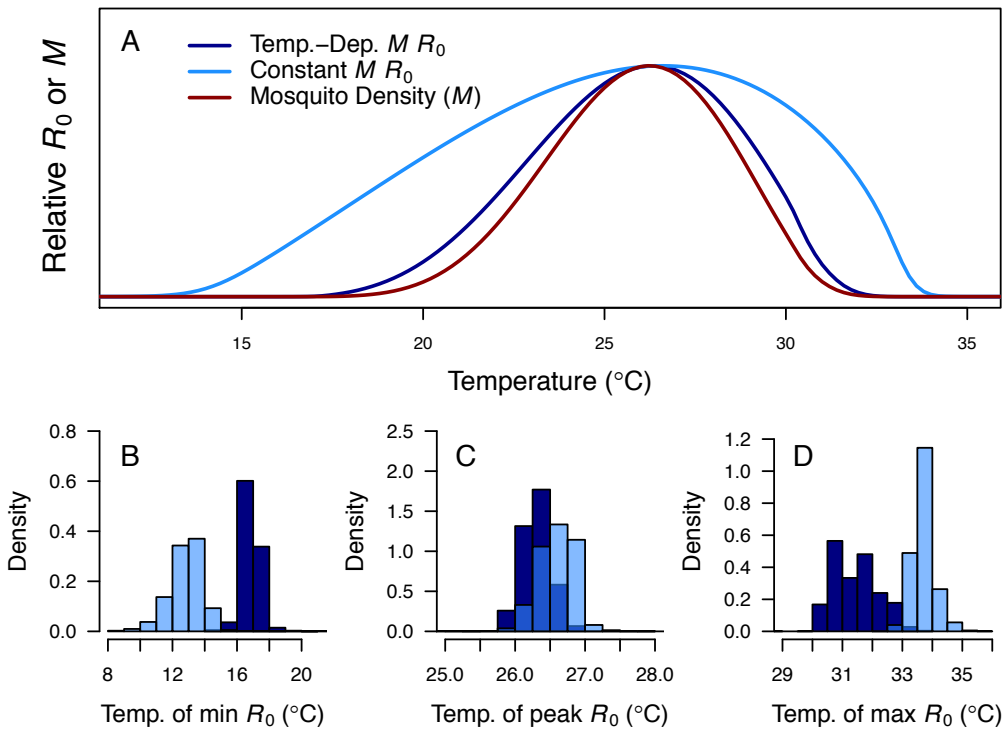

FIGURE 3: **Thermal response of relative R_0**. (A) Posterior means across temperature for constant M model (eq. 1, light blue) and temperature-dependent M model (eq. 2, dark blue). Predicted mosquito density (M) shown for comparison (red). The y-axis shows relative R_0 (or M) rather than absolute values, which would require additional information. Histograms of (B) the critical thermal minimum, (C) thermal optimum, and (D) critical thermal maximum temperatures for both models (same colors as in A).

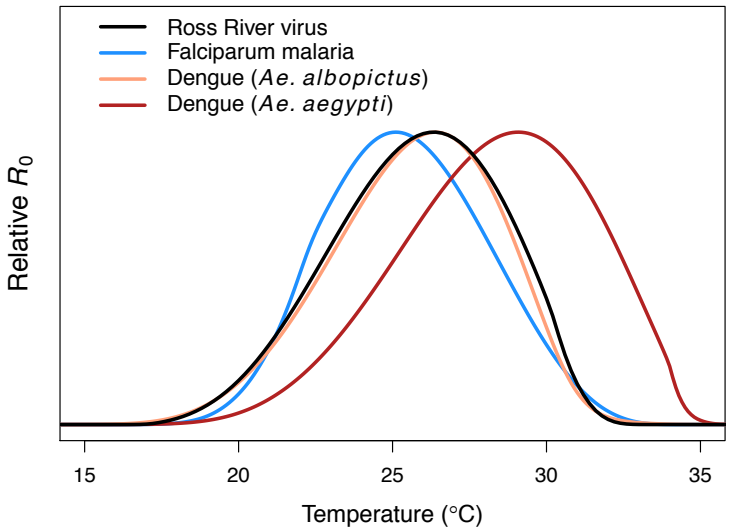

204

205 **FIGURE 4: Comparing the RRV R_0 model to other diseases:** malaria (blue, optimum =
206 25°C), Ross River virus (black, optimum = 26.4°C), dengue virus in *Ae. albopictus* (orange,
207 optimum = 26.4°C), and dengue virus in *Ae. agypti* (red, optimum = 29.1°C).

208

209 At the upper thermal limit fecundity (*EFD*) and adult lifespan (*lf*) constrain R_0, while at
210 the lower thermal limit fecundity, larval survival (*pLA*), egg survival (raft viability [*pRH*] and
211 survival within rafts [*nLR*]), and adult lifespan constrain R_0 (Fig. S6). All of these traits (except
212 adult lifespan) only occur in, and adult lifespan is quantitatively more important in, the
213 temperature-dependent *M* model. Correspondingly, uncertainty in these traits generated the most
214 uncertainty in R_0 at the respective thermal limits (Fig. S6C). The optimal temperature for R_0 was
215 most sensitive to the thermal response of adult lifespan. Near the optimum, most uncertainty in
216 R_0 was due to uncertainty in the thermal responses of adult lifespan, egg raft viability, and
217 fecundity. Substituting larval traits from alternative vectors or infection traits for Murray Valley
218 Encephalitis virus did not substantially alter the R_0 thermal response, since *Cx. annulirostris* life
219 history traits strongly constrained transmission (Fig. S5).

Temperature suitability for RRV transmission varies seasonally across Australia, based on the temperature-dependent *M* model (eq. 2) using monthly mean temperatures from WorldClim. In subtropical and temperate locations (Brisbane and further south), low temperatures force R_0 to zero for part of the year (Figs. 5A, 6). Monthly mean temperatures in these areas fall along the increasing portion of the R_0 curve for the entire year, so thermal suitability for transmission increases with temperature. By contrast, in tropical, northern Australia (Darwin and Cairns), the temperature remains suitable throughout the year (Figs. 5, 6). Darwin is the only major city where mean temperatures exceed the thermal optimum, and thereby depress transmission. Because most Australians live in southern, temperate areas, country-scale transmission is seasonal. As hypothesized *a priori*, human cases peak two months after population-weighted $R_0(T)$ (Fig. 7).

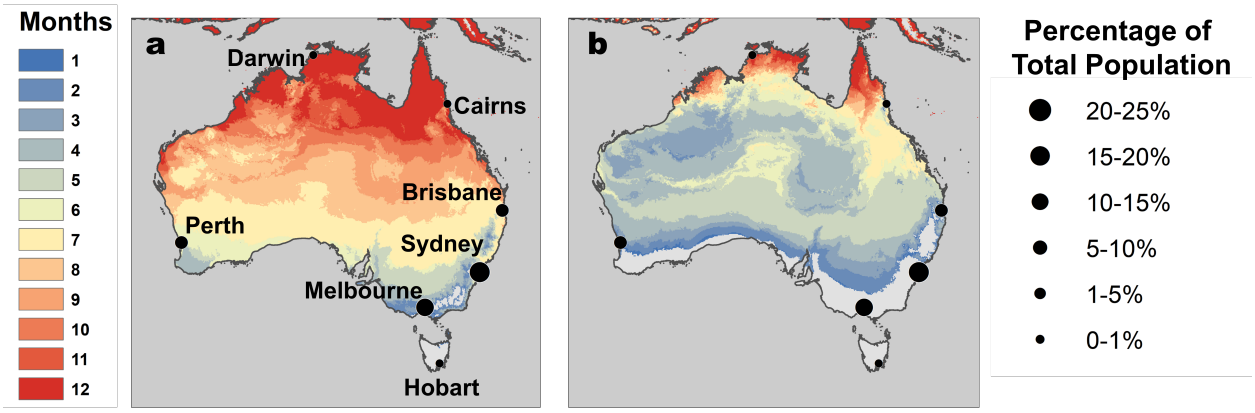

FIGURE 5: **RRV transmission potential from monthly mean temperatures**. Color indicates number of months where (A) relative R_0>0 and (B) relative R_0>0.5. Predictions are based on the posterior distribution medians. Points indicate selected cities (Fig. 5), scaled by the percent of total Australian population residing in each city.

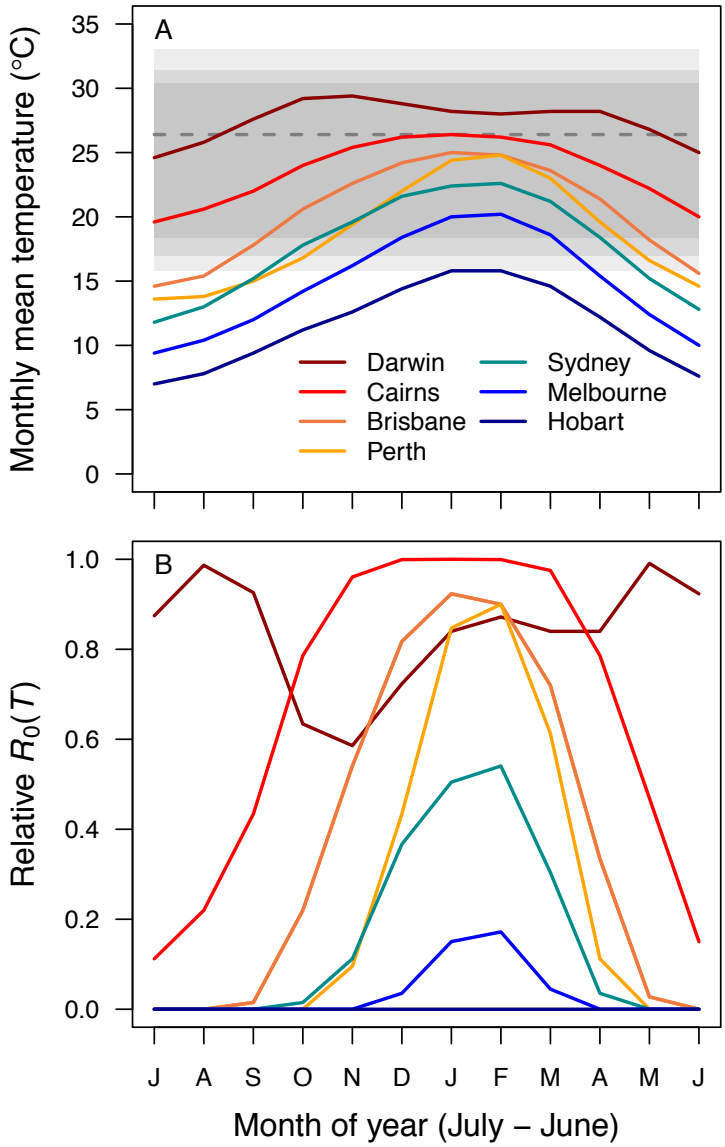

FIGURE 6: **Average seasonality of temperature and relative R_0 in Australian cities.** The selected cities span a latitudinal and temperature gradient (Darwin = dark red, Cairns = red, Brisbane = dark orange, Perth = light orange, Sydney = aqua, Melbourne = blue, Hobart = dark blue). The x-axis begins in July and ends in June (during winter). (A) Mean monthly temperatures. Shaded areas show temperature thresholds where R_0>0 for: outer 95% CI (light grey), median (medium grey), and inner 95% CI (dark grey). Dashed line shows median R_0 optimal temperature. (B) Temperature-dependent R_0.

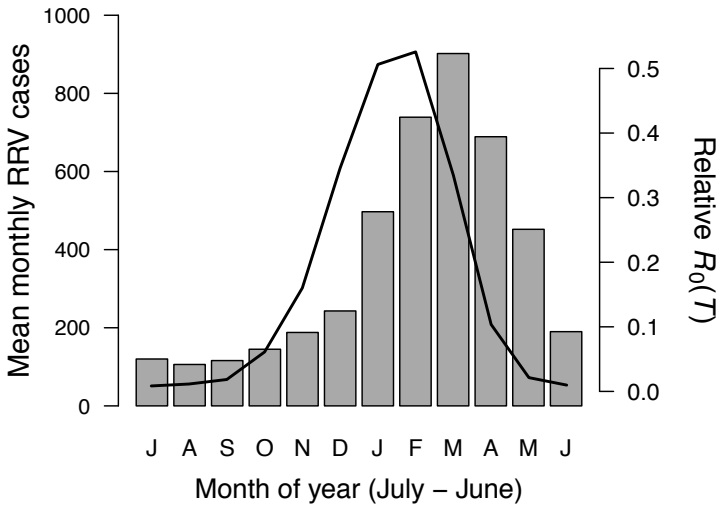

Figure 7: Seasonality of relative R_0 and RRV infections. Human cases aggregated nationwide from 1992-2013 (bars). Temperature-dependent R_0 weighted by population (line), calculated from Australia's 15 largest cities (76.6% of total population). The x-axis begins in July and ends in June (during winter). Cases peak two months after R_0, the *a priori* expected lag between temperature and reported cases.

DISCUSSION

In a warming world, it is critical to understand effects of temperature on transmission of mosquito-borne disease, particularly as new mosquito-borne pathogens emerge and spread worldwide. Identifying transmission optima and limits by characterizing nonlinear thermal responses, rather than simply assuming that transmission increases with temperature, can more accurately predict geographic, seasonal, and interannual variation in disease. Thermal responses vary substantially among diseases and vector species (Mordecai et al. 2013, 2017), yet we lack mechanistic models based on empirical, unimodal thermal responses for many diseases and vectors. Here, we parameterized a temperature-dependent model for transmission of RRV (Fig.

261 2) with data from two important vector species (*Cx. annulirostris* and *Ae. vigilax*; Fig. 1). The
262 optimal temperature for transmission is moderate (26-27ºC; Fig. 3), and largely determined by
263 the thermal response of adult mosquito lifespan (Fig. S6). Both low and high temperatures limit
264 transmission due to low mosquito fecundity and survival at all life stages (not just adults)—
265 thermal responses that are often ignored in transmission models (Fig. S6). Temperature explains
266 the geography of year-round endemic versus seasonally epidemic disease (Figs. 5, 6) and
267 accurately predicts the seasonality of human cases at the national scale (Fig. 7). Thus, the model
268 for RRV transmission provides a mechanistic link between geographic and seasonal variation in
269 temperature and broad-scale patterns of disease.

270 While the thermal response of RRV transmission generally matched those of other
271 mosquito-borne pathogens, there were some key differences. The moderate optimal temperature
272 for RRV (26-27ºC) fit within the range of thermal optima found for other diseases: malaria
273 transmission by *Anopheles* spp. at 25ºC, and dengue and other viruses by *Ae. aegypti* and *Ae.*
274 *albopictus* at 29ºC and 26ºC, respectively (Fig. 4) (Mordecai et al. 2013, 2017). For all of these
275 diseases, the specific temperature for optimal transmission was largely determined by the
276 thermal response of adult lifespan (Mordecai et al. 2013, 2017, Johnson et al. 2015). However,
277 the traits that set the thermal limits for RRV transmission differed from other systems. The lower
278 thermal limit for RRV was constrained by fecundity and survival at all stages while the upper
279 thermal limit was constrained by fecundity and adult lifespan. By contrast, thermal limits for
280 malaria transmission were set by parasite development rate at cool temperatures and egg-to-
281 adulthood survival at high temperatures (Mordecai et al. 2013). As with previous models, the
282 upper and lower thermal limits of RRV transmission are more uncertain than the optimum (Fig.
283 3) (Johnson et al. 2015, Mordecai et al. 2017), because trait responses are harder to measure near

284 their thermal limits where survival is low and development is slow or incomplete. Overall, our
285 results support a general pattern of intermediate thermal optima for transmission where the well-
286 resolved optimal temperature is driven by adult mosquito lifespan, but upper and lower thermal
287 limits are more uncertain and may be determined by unique traits for different vectors and
288 pathogens.

289 The trait thermal response data were limited in two keys ways. First, two traits (fecundity
290 and adult lifespan) had data from only three temperatures. We used priors derived from data
291 from other mosquito species to minimize over-fitting and better represent the true fit and
292 uncertainty (Fig. 2, versus uniform priors in Fig. S1). However, data from more temperatures
293 would increase our confidence in the fitted thermal responses. Second, no vector species had data
294 for all traits (Fig. 1), so we combined mosquito traits from *Cx. annulirostris* and pathogen
295 infection traits in *Ae. vigilax* to build composite R_0 models. Geographic and seasonal variation in
296 vector populations suggests that *Ae. camptorhynchus* and *Ae. vigilax* have different thermal
297 niches (cooler and warmer, respectively) and *Cx. annulirostris* has a broader thermal niche (Fig.
298 1) (Russell 1998). We need temperature-dependent trait data for more species to test the
299 hypothesis that these niche differences reflect the species' thermal responses. If true, the current
300 model, parameterized primarily with *Cx. annulirostris* trait responses, may not accurately predict
301 transmission by *Ae. camptorhynchus* and *Ae. vigilax*. Hypothesized species differences in
302 thermal niche could explain why RRV persists over a wide climatic and latitudinal gradient.
303 Thus, thermal response experiments with other RRV vectors are a critical area for future
304 research.

305 The temperature-dependent R_0 model provides a mechanistic explanation for
306 independently-observed patterns of RRV transmission across Australia. As predicted (Figs. 5, 6),

307 RRV is endemic in tropical Australia, with little seasonal variation in transmission potential due
308 to temperature, and seasonally epidemic in subtropical and temperate Australia (Weinstein
309 1997). The model also accurately predicts disease seasonality at the national scale (Fig. 7),
310 reproducing the *a priori* predicted lag (8-10 weeks) for temperature to affect reported human
311 cases (Hu et al. 2006, Jacups et al. 2008, Stewart Ibarra et al. 2013, Mordecai et al. 2017).
312 Further, RRV transmission by *Cx. annulirostris* in inland areas often moves south as
313 temperatures increase from spring into summer (Russell 1998), matching the model prediction
314 (Fig. 6). Although temperature is often invoked as a potential driver for such patterns, it is
315 difficult to establish causality from statistical inference alone, particularly if temperature and
316 disease both exhibit strong seasonality and could both be responding to another latent driver.
317 Thus, the mechanistic model is a critical piece of evidence linking temperature to patterns of
318 disease.

319 In addition to explaining broad-scale patterns, the unimodal thermal model explains
320 previously contradictory local-scale results. Specifically, statistical evidence for temperature
321 impacts on local time series of cases is mixed. RRV incidence is often—but not always—
322 positively associated with warmer temperatures (Tong and Hu 2001, Tong et al. 2002, 2004, Hu
323 et al. 2004, 2010, Jacups et al. 2008, Williams et al. 2009, Werner et al. 2012, Koolhof et al.
324 2017). However, variation in temperature impacts across space and time is expected from an
325 intermediate thermal optimum, especially when observed mean temperatures are near or cross
326 the optimum. The strongest statistical signal of temperature on disease is expected in temperate
327 regions where mean temperature varies along the rapidly rising portion of the R_0 curve (~20-
328 25°C). If mean temperatures vary both above and below the optimum (as in Darwin), important
329 effects of temperature may be masked in time series models that fit linear responses.

330 Additionally, if temperatures are always relatively suitable (as in tropical climates) or unsuitable
331 (as in very cool temperate climates), variation in disease may be due primarily to other factors. A
332 nonlinear mechanistic model is critical for estimating temperature impacts on transmission
333 because the effect of increasing temperature by a few degrees can have a positive, negligible, or
334 negative impact on R_0 along different parts of the thermal response curve. Although field-based
335 evidence for unimodal thermal responses in vector-borne disease is rare (but see Mordecai et al.
336 2013, Perkins et al. 2015, Peña-García et al. 2017), there is some evidence for high temperatures
337 constraining RRV transmission and vector populations: outbreaks were less likely with more
338 days above 35ºC in part of Queensland (Gatton et al. 2005) and populations of *Cx. annulirostris*
339 peaked at 25ºC and declined above 32ºC in Victoria (Dhileepan 1996). Future statistical analyses
340 of RRV cases may benefit from using a nonlinear function for temperature-dependent R_0 as a
341 predictor instead of raw temperature (Fig. 5B versus 5A).

342 Breeding habitat availability also drives mosquito abundance and mosquito-borne
343 disease. Local rainfall and river flow have been linked to the abundance of RRV vector species
344 (Tall et al. 2014) and RRV disease cases (Tong and Hu 2001, 2002a, Hu et al. 2004, Kelly-Hope
345 et al. 2004, Tong et al. 2004, Gatton et al. 2005, Jacups et al. 2008, Bi et al. 2009, Williams et al.
346 2009, Werner et al. 2012), as have unusually high tides in coastal areas with saltmarsh
347 mosquitoes (Tong and Hu 2002b, Tong et al. 2004, Jacups et al. 2008). Overlaying models of
348 species-specific breeding habitat with temperature-dependent models will better resolve the
349 geographic and seasonal distribution of RRV transmission. R_0 peaked at similar temperatures
350 whether or not we assumed mosquito abundance was temperature-dependent (eq. 1 versus eq. 2);
351 however, the range of suitable temperatures was much wider for the model that assumed a
352 temperature-independent mosquito population (Fig. 3). Since breeding habitat can only impact

353 vector populations when temperatures do not exclude them, it is critical to consider thermal
354 constraints on mosquito abundance, even when breeding habitat is considered a stronger driver.
355 Nonetheless, many mechanistic, temperature-dependent models of vector-borne disease
356 transmission do not include thermal effects on vector density (Martens et al. 1997, Craig et al.
357 1999, Caminade et al. 2017, Paull et al. 2017, Hamlet et al. 2018). Our results demonstrate that
358 the decision to exclude these relationships can have a critical impact on model results, especially
359 near thermal limits.

360 Several important gaps remain in our understanding of RRV thermal ecology, in addition
361 to the need for trait thermal response data for more vector species. First, the R_0 model needs to be
362 more rigorously validated using time series of cases to determine the importance of temperature
363 at finer spatiotemporal scales. These analyses should incorporate daily and seasonal temperature
364 variation (Paaijmans et al. 2010) and integrate species-specific drivers of breeding habitat
365 availability, like rainfall and tidal patterns. Second, translating environmental suitability for
366 transmission into human cases also depends on disease dynamics in reservoir host populations
367 and their impact on immunity. For instance, in Western Australia heavy summer rains can fail to
368 initiate epidemics when low rainfall in the preceding winter depresses recruitment of susceptible
369 juvenile kangaroos (Mackenzie et al. 2000). By contrast, large outbreaks occur in southeastern
370 Australia when high rainfall follows a dry year, presumably from higher transmission within
371 relatively unexposed reservoir populations (Woodruff et al. 2002). Building vector species-
372 specific R_0 models and integrating thermal ecology with other drivers are important next steps
373 for forecasting variation in RRV transmission.

374 Nonlinear thermal responses are particularly important for predicting how transmission
375 will change under future climate regimes. Climate warming will likely increase the geographic

and seasonal range of transmission potential in temperate, southern Australia where most Australians live. However, climate change will likely decrease transmission potential in tropical areas like Darwin, where moderate warming (~3ºC) would push temperatures above the upper thermal limit for transmission for most of the year (Fig. 5). However, the extent of climate-driven declines in transmission will depend on how much *Cx. annulirostris* and *Ae. vigilax* can adapt to extend their upper thermal limits and whether warmer-adapted vector species (e.g., *Ae. aegypti* and potentially *Ae. polynesiensis*) can invade and sustain RRV transmission cycles. Thus, we can predict the response of RRV transmission by current vector species to climate change based on these trait thermal responses. However, future disease dynamics will also depend on vector adaptation, potential vector species invasions, and climate change impacts on sea level and precipitation that drive vector habitat availability.

METHODS

Temperature-Dependent R_0 Models

We used two R_0 models: 'Constant *M* Model' (eq. 1) assumes mosquito density (*M*) does not depend on temperature (equation from Dietz 1993); 'Temperature-Dependent *M* Model' (eq. 2) assumes temperature drives mosquito density and includes vector life history trait thermal responses (Parham and Michael 2010, Mordecai et al. 2013, 2017).

Constant *M* Model: $$R_0(T) = \left(\frac{a(T)^2 bc(T) e^{-\frac{\mu(T)}{PDR(T)}} M}{N\, r\, \mu(T)} \right)^{1/2} \qquad \text{eq. 1}$$

Temperature-dependent *M* Model: $$R_0(T) = \left(\frac{a(T)^2 bc(T) e^{-\frac{\mu(T)}{PDR(T)}} EFD(T) p_{EA} MDR(T)}{N\, r\, \mu(T)^3} \right)^{1/2} \qquad \text{eq. 2}$$

396 In both equations, (T) indicates a parameter depends on temperature, a is mosquito biting
397 rate, bc is vector competence (proportion of mosquitoes becoming infectious post-exposure), μ is
398 adult mosquito mortality rate (adult lifespan, $lf = 1/\mu$), PDR is parasite development rate ($PDR =$
399 $1/EIP$, the extrinsic incubation period), N is human density, and r is the recovery rate at which
400 humans become immune (all rates are measured in days^{-1}). The latter two terms do not depend
401 on temperature. In the temperature-dependent M model, mosquito density (M) depends on
402 fecundity (EFD, eggs per female per day), proportion surviving from egg-to-adulthood (p_{EA}), and
403 mosquito development rate (MDR), divided by the square of adult mortality rate (μ) (Parham and
404 Michael 2010). We calculated p_{EA} as the product of the proportion of egg rafts that hatch (pRH),
405 the number of larvae per raft (nLR, scaled by the maximum at any temperature to calculate
406 proportional egg survival within-rafts), and the proportion of larvae surviving to adulthood (p_{LA}).
407 We fit thermal responses of traits in the R_0 models to previously published data (Table
408 S2) using Bayesian inference with the 'r2jags' package (Plummer 2003, Su and Yajima 2009) in
409 R (R Core Team 2017). Traits with asymmetrical thermal responses were fit as Brière functions:
410 $qT(T–T_0)(T_{max}–T)^{1/2}$ (Brière et al. 1999). Traits with symmetrical thermal responses were fit as
411 quadratic functions: $-q(T–T_0)(T–T_{max})$. In both functions of temperature (T), T_0 and T_{max} are the
412 critical thermal minimum and maximum, respectively, and q is a rate parameter. For priors we
413 used gamma distributions with hyperparameters derived from thermal responses fit to data from
414 other mosquito species (Table S4), allowing us to more accurately represent the fit and
415 uncertainty. Our data did not include declining trait values at high temperatures for biting rate (a)
416 and parasite development rate (PDR). Nonetheless, data from other mosquito species (Mordecai
417 et al. 2013, 2017) and principles of thermal biology (Dell et al. 2011) imply these traits must
418 decline at high temperatures. Thus, for those traits we included an artificial data point where the

trait value approached zero at a very high temperature (40ºC), allowing us to fit the Brière function. We used strongly informative priors to limit the effect of these traits on the upper thermal limit of R_0 (by constraining them to decline near 40ºC). For comparison, we also fit all thermal responses with uniform priors (Fig. S1); these results illustrate how the priors impacted the results.

Sensitivity and uncertainty analyses

We conducted sensitivity and uncertainty analyses of the temperature-dependent M model (eq. 2) to understand how trait thermal responses shape the thermal response of R_0. We examined the sensitivity of R_0 two ways. First, we evaluated the impact of each trait by setting it constant while allowing all other traits to vary with temperature. Second, we calculated the partial derivative of R_0 with respect to each trait across temperature ($\partial R_0/\partial X \cdot \partial X/\partial T$ for trait X and temperature T; Appendix). To understand what data would most improve the model, we also calculated the proportion of total uncertainty in R_0 due to each trait across temperature. First, we propagated posterior samples from all trait thermal response distributions through to $R_0(T)$ and calculated the width of the 95% highest posterior density interval (HPD interval; a type of credible interval) of this distribution at each temperature: the 'full $R_0(T)$ uncertainty'. Next, we sampled each trait from its posterior distribution while setting all other trait thermal responses to their posterior medians, and calculated the posterior distribution of $R_0(T)$ and the width of its 95% HPD interval across temperature: the 'single-trait $R_0(T)$ uncertainty'. Finally, we divided each single-trait $R_0(T)$ uncertainty by the full $R_0(T)$ uncertainty.

441 *Field Observations: Seasonality of Temperature-Dependent R_0 Across Australia*

442 We took monthly mean temperatures from WorldClim for seven cities spanning a
443 latitudinal and temperature gradient (from tropical North to temperate South: Darwin, Cairns,
444 Brisbane, Perth, Sydney, Melbourne, and Hobart) and calculated the posterior median $R_0(T)$ for
445 each month at each location. We also compared the seasonality of a population-weighted $R_0(T)$
446 and nationally aggregated RRV cases. We used 2016 estimates for the fifteen most populous
447 urban areas, which together contain 76.6% of Australia's population (Australian Bureau of
448 Statistics 2017). We calculated $R_0(T)$ for each location (as above) and estimated a population-
449 weighted average. We compared this country-scale estimate of $R_0(T)$ with data on mean monthly
450 human cases of RRV nationwide from 1992-2013 obtained from the National Notifiable
451 Diseases Surveillance System.

452 We expected a time lag between temperature and reported human cases as mosquito
453 populations increase, bite humans and reservoir hosts, acquire RRV, become infectious, and bite
454 subsequent hosts; after an incubation period hosts (potentially) become symptomatic, seek
455 treatment, and report cases. Empirical work on dengue vectors in Ecuador identified a six-week
456 time lag between temperature and mosquito oviposition (Stewart Ibarra et al. 2013). Subsequent
457 mosquito development and incubation periods in mosquitoes and humans likely add another 2-4
458 week lag before cases appear, resulting in an 8-10 week lag between temperature and observed
459 cases (Hu et al. 2006, Jacups et al. 2008, Mordecai et al. 2017). With monthly case data, we
460 hypothesize a two-month time lag between $R_0(T)$ and RRV disease cases.

461

462 *Mapping Temperature-Dependent R_0 Across Australia*

463 To illustrate temperature suitability for RRV transmission across Australia, we mapped
464 the number of months for which relative $R_0(T)>0$ and >0.5 for the posterior median, 2.5%, and
465 97.5% credibility bounds (Fig. S7) for the temperature-dependent M model (eq. 2). We
466 calculated $R_0(T)$ at 0.2°C increments and projected it onto the landscape for monthly mean
467 temperatures from WorldClim data at a 5-minute resolution (approximately 10km^2 at the
468 equator). Climate data layers were extracted for the geographic area, defined using the Global
469 Administrative Boundaries Databases (GADM 2012). We performed map calculations and
470 manipulations in R with packages 'raster' (Hijmans 2016), 'maptools' (Bivand and Lewin-Koh
471 2017), and 'Rgdal' (Bivand et al. 2017), and rendered GeoTiffs in ArcGIS version 10.3.1.
472

473 **ACKNOWLEDGEMENTS**

474 We thank Leah Johnson and Matt Thomas for comments and Cameron Webb for posting
475 the RRV case data (https://cameronwebb.wordpress.com/2014/04/09/why-is-mosquito-borne-
476 disease-risk-greater-in-autumn/).
477

478 **FUNDING**

479 All authors were supported by the National Science Foundation (DEB-1518681;
480 https://nsf.gov/). EAM was supported by the NSF (DEB-1640780; https://nsf.gov/), the Stanford
481 Woods Institute for the Environment (https://woods.stanford.edu/research/environmental-
482 venture-projects), and the Stanford Center for Innovation in Global Health
483 (http://globalhealth.stanford.edu/research/seed-grants.html).
484

485 **REFERENCES**

486 Australian Bureau of Statistics. 2017. 3218.0 - Regional Population Growth, Australia, 2016.
487 Canberra.
488 Barton, P. S., J. G. Aberton, and B. H. Kay. 2004. Spatial and temporal definition of
489 *Ochlerotatus camptorhynchus* (Thomson) (Diptera: Culicidae) in the Gippsland Lakes
490 system of eastern Victoria. Australian Journal of Entomology 43:16–22.
491 Bi, P., J. E. Hiller, a S. Cameron, Y. Zhang, and R. Givney. 2009. Climate variability and Ross
492 River virus infections in Riverland, South Australia, 1992-2004. Epidemiology and
493 infection 137:1486–93.
494 Biggs, A. J. W., and P. Mottram. 2008. Links between dryland salinity, mosquito vectors, and
495 Ross River Virus disease in southern inland Queensland—an example and potential
496 implications. Soil Research 46:62–66.
497 Bivand, R., T. Keitt, and B. Rowlingson. 2017. rgdal: Bindings for the "Geospatial" Data
498 Abstraction Library.
499 Bivand, R., and N. Lewin-Koh. 2017. maptools: Tools for Reading and Handling Spatial
500 Objeccts.
501 Brière, J.-F., P. Pracros, A.-Y. Le Roux, and J.-S. Pierre. 1999. A Novel Rate Model of
502 Temperature-Dependent Development for Arthropods. Environmental Entomology 28:22–
503 29.
504 Caminade, C., Turner, J., Metelmann, S., Hesson, J.C., Blagrove, M.S., Solomon, T., Morse,
505 A.P. and Baylis, M., 2017. Global risk model for vector-borne transmission of Zika virus
506 reveals the role of El Niño 2015. Proceedings of the National Academy of Sciences,
507 114(1):119-124.
508 Carver, S., H. Spafford, A. Storey, and P. Weinstein. 2009. Dryland Salinity and the Ecology of
509 Ross River Virus: The Ecological Underpinnings of the Potential for Transmission. Vector-
510 Borne and Zoonotic Diseases 9:611–622.
511 Claflin, S. B., and C. E. Webb. 2015. Ross River Virus: Many Vectors and Unusual Hosts Make
512 for an Unpredictable Pathogen. PLoS Pathogens 11:1–6.
513 Clements, A. N., and G. D. Paterson. 1981. The Analysis of Mortality and Survival Rates in
514 Wild Populations of Mosquitoes. Journal of Applied Ecology 18:373–399.

515 Craig, M.H., Snow, R.W. and le Sueur, D., 1999. A climate-based distribution model of malaria
516 transmission in sub-Saharan Africa. Parasitology today, 15(3):105-111.
517 Dell, A. I., S. Pawar, and V. M. Savage. 2011. Systematic variation in the temperature
518 dependence of physiological and ecological traits. Proceedings of the National Academy of
519 Sciences 108:10591–10596.
520 Dhileepan, K. 1996. Mosquito seasonality and arboviral disease incidence in Murray valley,
521 southeast Australia. Medical and Veterinary Entomology 10:375–384.
522 Dietz, K. 1993. The estimation of the basic reproduction number for infectious diseases.
523 Statistical Methods in Medical Research 2:23–41.
524 Flies, E. J., C. L. Lau, S. Carver, and P. Weinstein. 2018. Another Emerging Mosquito-Borne
525 Disease? Endemic Ross River Virus Transmission in the Absence of Marsupial Reservoirs.
526 BioScience.
527 GADM. 2012. GADM database of Global Administrative Boundaries, version 2.0.
528 Gatton, M. L., B. H. Kay, and P. A. Ryan. 2005. Environmental predictors of Ross River virus
529 disease outbreaks in Queensland, Australia. Am J Trop Med Hyg 72:792–799.
530 Hamlet, A., K. Jean, W. Perea, S. Yactayo, J. Biey, M. Van Kerkhove, N. Ferguson, and T.
531 Garske. 2018. The seasonal influence of climate and environment on yellow fever
532 transmission across Africa. PLOS Neglected Tropical Diseases 12:e0006284.
533 Harley, D., A. Sleigh, and S. Ritchie. 2001. Ross River Virus Transmission, Infection, and
534 Disease: a Cross-Disciplinary Review. Clinical Microbiology Reviews 14:909–932.
535 Hijmans, R. J. 2016. raster: Geographic Data Analysis and Modeling.
536 Hu, W., A. Clements, G. Williams, S. Tong, and K. Mengersen. 2010. Bayesian spatiotemporal
537 analysis of socio-ecologic drivers of Ross River virus transmission in Queensland,
538 Australia. American Journal of Tropical Medicine and Hygiene 83:722–728.
539 Hu, W., N. Nicholls, M. Lindsay, P. Dale, A. J. McMichael, J. S. Mackenzie, and S. Tong. 2004.
540 Development of a predictive model for ross river virus disease in Brisbane, Australia. Am J
541 Trop Med Hyg 71:129–137.
542 Hu, W., S. Tong, K. Mengersen, B. Oldenburg, and P. Dale. 2006. Mosquito species (Diptera:
543 Culicidae) and the transmission of Ross River virus in Brisbane, Australia. Journal of
544 Medical Entomology 43:375–381.
545 Jacups, S. P., J. Carter, N. Kurucz, J. McDonnell, and P. I. Whelan. 2015. Determining

546 meteorological drivers of salt marsh mosquito peaks in tropical northern Australia. Journal
547 of Vector Ecology 40:277–281.
548 Jacups, S. P., P. I. Whelan, P. G. Markey, S. J. Cleland, G. J. Williamson, and B. J. Currie. 2008.
549 Predictive indicators for Ross River virus infection in the Darwin area of tropical northern
550 Australia, using long-term mosquito trapping data. Tropical Medicine and International
551 Health 13:943–952.
552 Johnson, L. R., T. Ben-Horin, K. D. Lafferty, A. McNally, E. Mordecai, K. P. Paaijmans, S.
553 Pawar, and S. J. Ryan. 2015. Understanding uncertainty in temperature effects on vector-
554 borne disease: A Bayesian approach. Ecology 96:203–213.
555 Kay, B. H., and C. D. Jennings. 2002. Enhancement or Modulation of the Vector Competence of
556 *Ochlerotatus vigilax* (Diptera: Culicidae) for Ross River Virus by Temperature. Journal of
557 Medical Entomology 39:99–105.
558 Kelly-Hope, L. A., D. M. Purdie, and B. H. Kay. 2004. Differences in Climatic Factors Between
559 Ross River Virus Disease Outbreak and Nonoutbreak Years. J. Med. Entomol 41:1116–
560 1122.
561 Klapsing, P., J. D. MacLean, S. Glaze, K. L. McClean, M. A. Drebot, R. S. Lanciotti, and G. L.
562 Campbell. 2005. Ross river virus disease reemergence, Fiji, 2003-2004. Emerging
563 Infectious Diseases 11:613–615.
564 Kokkinn, M. J., D. J. Duval, and C. R. Williams. 2009. Modelling the ecology of the coastal
565 mosquitoes *Aedes vigilax* and *Aedes camptorhynchus* at Port Pirie, South Australia. Medical
566 and Veterinary Entomology 23:85–91.
567 Koolhof, I. S., S. Bettiol, and S. Carver. 2017. Fine-temporal forecasting of outbreak probability
568 and severity: Ross River virus in Western Australia. Epidemiology and Infection 145:2949–
569 2960.
570 Liu-Helmersson, J., H. Stenlund, A. Wilder-Smith, and J. Rocklöv. 2014. Vectorial capacity of
571 *Aedes aegypti*: Effects of temperature and implications for global dengue epidemic
572 potential. PLoS ONE 9.
573 Mackenzie, J. S., M. D. Lindsay, and A. K. Broom. 2000. The effect of climate and weather on
574 the transmission of Ross River and Murray Valley encephalitis viruses. Microbiology
575 Australia 21:20–25.

576 Martens, W.J., Jetten, T.H. and Focks, D.A., 1997. Sensitivity of malaria, schistosomiasis and
577 dengue to global warming. Climatic change, 35(2):145-156.
578 McDonald, G., I. W. McLaren, G. P. Shelden, and I. R. Smith. 1980. The effect of temperature
579 on the population growth potential of *Culex annulirostris* Skuse (Diptera: Culicidae).
580 Australian Journal of Ecology 5:379–384.
581 Mordecai, E. A., J. M. Cohen, M. V. Evans, P. Gudapati, L. R. Johnson, C. A. Lippi, K.
582 Miazgowicz, C. C. Murdock, J. R. Rohr, S. J. Ryan, V. Savage, M. S. Shocket, A. Stewart
583 Ibarra, M. B. Thomas, and D. P. Weikel. 2017. Detecting the impact of temperature on
584 transmission of Zika, dengue, and chikungunya using mechanistic models. PLOS Neglected
585 Tropical Diseases 11:e0005568.
586 Mordecai, E. A., K. P. Paaijmans, L. R. Johnson, C. Balzer, T. Ben-Horin, E. de Moor, A.
587 McNally, S. Pawar, S. J. Ryan, T. C. Smith, and K. D. Lafferty. 2013. Optimal temperature
588 for malaria transmission is dramatically lower than previously predicted. Ecology letters
589 16:22–30.
590 Mottram, P., B. H. Kay, and D. S. Kettle. 1986. The effect of temperature on eggs and immature
591 Stages of *Culex annulirostris* Skuse (Diptera: Culicidae). Australian Journal of Entomology
592 25:131–136.
593 Paaijmans, K. P., S. Blanford, A. S. Bell, J. I. Blanford, A. F. Read, and M. B. Thomas. 2010.
594 Influence of climate on malaria transmission depends on daily temperature variation.
595 Proceedings of the National Academy of Sciences of the United States of America
596 107:15135–9.
597 Parham, P. E., and E. Michael. 2010. Modeling the effects of weather and climate change on
598 malaria transmission. Environmental Health Perspectives 118:620–626.
599 Paull, S. H., D. E. Horton, M. Ashfaq, D. Rastogi, L. D. Kramer, N. S. Diffenbaugh, and A. M.
600 Kilpatrick. 2017. Drought and immunity determine the intensity of West Nile virus
601 epidemics and climate change impacts. Proceedings of the Royal Society B: Biological
602 Sciences 284:20162078.
603 Peña-García, V. H., O. Triana-Chávez, and S. Arboleda-Sánchez. 2017. Estimating Effects of
604 Temperature on Dengue Transmission in Colombian Cities. Annals of Global Health
605 83:509–518.
606 Perkins, T. A., C. J. E. Metcalf, B. T. Grenfell, and A. J. Tatem. 2015. Estimating Drivers of

Autochthonous Transmission of Chikungunya Virus in its Invasion of the Americas. PLoS Current Outbreaks 1.

Plummer, M. 2003. JAGS: A program for analysis of Bayesian graphical models using Gibbs sampling. Proceedings of the 3rd International Workshop on Distributed Statistical Computing:1–10.

R Core Team. 2017. R: A language and for statistical computing. R Foundation for Statistical Computing, Vienna, Austria.

Rae, D. J. 1990. Survival and development of the immature stages of *Culex annulirostris* (Diptera: Culicidae) at the Ross River Dam in tropical eastern Australia. J Med Entomol 27:756–762.

Rogers, D. J., and S. E. Randolph. 2006. Climate Change and Vector-Borne Diseases. Advances in Parasitology 62:345–381.

Russell, R. C. 1986. *Culex Annulirostris* Skuse (Diptera: Culicidae) at Appin, N.S.W.—bionomics and behavior. Australian Journal of Entomology 25:103–109.

Russell, R. C. 1998. Mosquito-borne arboviruses in Australia: the current scene and implications of climate change for human health. International Journal for Parasitology 28:955–969.

Russell, R. C. 2002. Ross River Virus: Ecology and Distribution. Annal Reviews Entomology 47:1–31.

Siraj, A. S., M. J. Bouma, M. Santos-Vega, A. K. Yeshiwondim, D. S. Rothman, D. Yadeta, P. C. Sutton, and M. Pascual. 2015. Temperature and population density determine reservoir regions of seasonal persistence in highland malaria. Proceedings of the Royal Society B: Biological Sciences 282:20151383.

Stewart Ibarra, A. M., and R. Lowe. 2013. Climate and non-climate drivers of dengue epidemics in southern coastal Ecuador. American Journal of Tropical Medicine and Hygiene 88:971–981.

Stewart Ibarra, A. M., S. J. Ryan, E. Beltrán, R. L. Mejía, M. Silva, Á. Muñoz, A. M. S. Ibarra, S. J. Ryan, E. Beltrá N, R. L. Mejía, M. Silva, and N. Muñ Oz. 2013. Dengue Vector Dynamics (*Aedes aegypti*) Influenced by Climate and Social Factors in Ecuador: Implications for Targeted Control. PLoS ONE 8:e78263.

Su, Y.-S., and M. Yajima. 2009. R2jags: A Package for Running jags from R.

Tall, J. A., M. L. Gatton, and S. Tong. 2014. Ross River Virus Disease Activity Associated With

638 Naturally Occurring Nontidal Flood Events in Australia: A Systematic Review. Journal of
639 Medical Entomology 51:1097–1108.
640 Tong, S., P. Bi, K. Donald, and A. J. McMichael. 2002. Climate variability and Ross River virus
641 transmission. Journal of Epidemiology & Community Health 56:617–621.
642 Tong, S., and W. Hu. 2001. Climate variation and incidence of Ross River virus in Cairns,
643 Australia: a time-series analysis. Environmental Health Perspectives 109:1271–1273.
644 Tong, S., and W. Hu. 2002a. Different responses of Ross River virus to climate variability
645 between coastline and inland cities in Queensland, Australia. Occup Environ Med 59:739–
646 744.
647 Tong, S., and W. Hu. 2002b. Different responses of Ross River virus to climate. Occup Environ
648 Med 59:739–744.
649 Tong, S., W. Hu, and A. J. McMichael. 2004. Climate variability and Ross River virus
650 transmission in Townsville Region, Australia, 1985-1996. Tropical Medicine and
651 International Health 9:298–304.
652 Weinstein, P. 1997. An ecological approach to public health intervention: Ross River virus in
653 Australia. Environ Health Perspect 105:364–366.
654 Werner, A. K., S. Goater, S. Carver, G. Robertson, G. R. Allen, and P. Weinstein. 2012.
655 Environmental drivers of Ross River virus in southeastern Tasmania, Australia: towards
656 strengthening public health interventions. Epidemiology and Infection 140:359–371.
657 Wesolowski, A., T. Qureshi, M. F. Boni, P. R. Sundsøy, M. A. Johansson, S. B. Rasheed, K.
658 Engø-Monsen, and C. O. Buckee. 2015. Impact of human mobility on the emergence of
659 dengue epidemics in Pakistan. Proceedings of the National Academy of
660 Sciences:201504964.
661 Williams, C. R., S. R. Fricker, and M. J. Kokkinn. 2009. Environmental and entomological
662 factors determining Ross River virus activity in the River Murray Valley of South Australia.
663 Australian and New Zealand Journal of Public Health 33:284–288.
664 Woodruff, R. E., C. S. Guest, M. G. Garner, N. Becker, J. Lindesay, T. Carvan, and K. Ebi.
665 2002. Predicting Ross River virus epidemics from regional weather data. Epidemiology
666 13:384–393.
667

Appendix S1 *Additional Notes, Tables, Figures, Methods, and References*

Notes: Notes on (1) mosquito nomenclature, (2) the use of medians versus means in the trait and R_0 thermal responses, and (3) data digitization.

Tables:

Table S1: Locations and data sources for Fig. 1, vector species implicated in RRV outbreaks.

Table S2: Trait thermal response functions and data sources for *Cx. annulirostris* and Ross River virus (in *Ae. vigilax*) traits (Fig. 2, Fig. S1).

Table S3: Trait thermal response functions and data sources for Murray Valley Encephalitis virus and additional vector species (*Ae. notoscriptus* and *Ae. camptorhynchus*).

Table S4: Trait thermal response functions and data sources used to parameterize priors for mosquito and virus traits (Fig. 2, Fig. S2, Fig. S3, Fig. S4).

Figures:

Figure S1: Thermal responses of *Cx. annulirostris* and Ross River virus (in *Ae. vigilax*) traits fit with uniform priors.

Figure S2: Thermal responses for larval survival and development rate for *Ae. camptorhynchus*.

Figure S3: Thermal responses for larval survival and development rate for *Ae. notoscriptus*.

Figure S4: Thermal responses for Murray Valley Encephalitis virus (MVEV) traits in *Cx. annulirostris*.

Figure S5: Additional R_0 and mosquito density model results: R_0 thermal responses for RRV with data-informed priors and uniform priors; R_0 thermal responses for RRV with larval traits from alternative hosts; R_0 thermal responses for MVEV.

Figure S6: Sensitivity and uncertainty analyses for RRV R_0 model.

Figure S7: Maps showing confidence intervals for Fig. 5A (months where $R_0 > 0$ with 2.5% and 97.5% of the posterior probability).

Figure S8: Example showing mean versus median of R_0 thermal response posterior distribution.

Methods: Partial derivatives for sensitivity analysis

Additional methods for survival and fecundity data from McDonald *et al.* 1980

References: References for Appendix S1

Mosquito nomenclature

In 2000, there was a proposed shift in mosquito taxonomy: several subgenera within the genus *Aedes* were elevated to genus status (Wilkerson *et al.* 2015). This move affected the two saltmarsh mosquitoes included in this study, *Aedes vigilax* and *Aedes camptorhynchus*, which for a time were called *Ochlerotataus vigilax* and *Ochlerotatus camptorhynchus* by some researchers. More recently, there has been a consensus to move back to the previous naming system, so we use *Aedes* here, although many of the papers we cite use *Ocherlotatus* instead.

The use of means versus medians in thermal responses

Bayesian inference produces output in the form of posterior distributions rather than a single estimated value. Because these distributions can be non-normal and asymmetric, best practice is to report medians rather than means, since medians are less sensitive to outlying values in extended tails. In this study, we report median parameter values and use median predicted values for downstream analyses (e.g., sensitivity and uncertainty analyses, predictions using weather data). However, we plot mean values in the figures because they show a smoother and more visually intuitive representation of where trait and R_0 thermal responses go to zero at the upper thermal limits. The means and medians are not substantially different, except at these thermal limits (Fig S8).

Data digitization

We digitized previously published data using a free web-based tool called Webplot digitizer available at: https://automeris.io/WebPlotDigitizer/.

TABLE S1: **Mosquito species implicated in RRV outbreaks** (Fig. 1). Location and year of RRV disease outbreaks and mosquito species identified as likely vectors based on the collection of field specimens. Only the six most important mosquito species are included.

Location	Year(s)	Species	Citation(s)
Queensland			
Cairns	1996-8	*Ae. vigilax* *Ae. notoscriptus* *Cx. annulirostris*	F
Shoalwater Bay Training Area	1997-8	*Ae. vigilax* *Cx. annulirostris*	I, E
Brisbane + surrounding area	1994, 1996	*Ae. vigilax* *Ae. notoscriptus* *Cx. annulirostris*	I, S, X
Warwick	2004	*Ae. vigilax*	A
New South Wales			
Sydney suburbs	1999	*Ae. notoscriptus* *Cx. annulirostris*	B
Bateman's Bay	1985-8	*Ae. vigilax*	U
Southern inland areas	1983-4, 1993	*Cx. annulirostris*	G, I, P
Victoria			
Gippsland region	1988-9	*Ae. camptorhynchus*	G, C, V
Murray River valley area	1991-1995	*Cx. annulirostris*	I, D
South Australia			
Murray River	1991-3	*Cx. annulirostris*	I, V
Western Australia			
Wheatbelt region	1992	*Ae. camptorhynchus*	O
Peel region + Bunbury	1995-6	*Ae. camptorhynchus* *Ae. vigilax*	I, N
Perth	1991-2	*Ae. camptorhynchus*	G, K
Gascoyne region (coastal)	1992	*Ae. vigilax*	M
Pilbara region (coastal)	1992	*Ae. vigilax*	L
Kimberley region (inland)	1982-6	*Cx. annulirostris* *Ae. normanensis*	M
Northern Territory			
Darwin	1991-2006	*Ae. vigilax* *Ae. notoscriptus* *Cx. annulirostris*	H, Z, AB
Nhulunbuy	1991-2	*Ae. vigilax*	R, Z
Alice Springs + surrounding area	1995	*Cx. annulirostris* *Ae. normanensis*	W, AA
Tasmania			
Hobart + surrounding area	1991	*Ae. camptorhynchus*	G, Q
Pacific Island nations			
American Samoa	NA	*Ae. polynesiensis*	J, Y
Cook Islands	1981	*Ae. polynesiensis*	T

Table S1 Citation key:

(A: Biggs & Mottram 2008)
(B: Brokenshire *et al.* 2000)
(C: Campbell *et al.* 1989)
(D: Dhileepan 1996)
(E: Frances *et al.* 2004)
(F: Harley *et al.* 2000)
(G: Harley *et al.* 2001)
(H: Jacups *et al.* 2008)
(I: Kelly-Hope *et al.* 2004)
(J: Lau *et al.* 2017)
(K: Lindsay *et al.* 1992)
(L: Lindsay *et al.* 1993b)
(M: Lindsay *et al.* 1993a)
(N: Lindsay *et al.* 1996)
(O: Lindsay *et al.* 2007)
(P: McDonnell *et al.* 1994)
(Q: McManus *et al.* 1992)
(R: Merianos *et al.* 1992)
(S: Ritchie *et al.* 1997)
(T: Rosen *et al.* 1981)
(U: Russell *et al.* 1991)
(V: Russell 1994)
(W: Russell 2002)
(X: Ryan *et al.* 2000)
(Y: Schmaedick *et al.* 2008)
(Z: Whelan *et al.* 1992)
(AA: Whelan *et al.* 1995)
(AB: Whelan *et al.* 1997)

TABLE S2: Trait thermal response functions and data sources for Ross River virus R_0 models (eqs. 1 and 2). 'Par.' = model parameter. Results are given for fits from data-informed priors. Asymmetrical responses fit with Brière function (**B**): $B(T) = qT(T - T_0)(T_{max} - T)^{1/2}$; symmetrical responses fit with quadratic function (**Q**): $Q(T) = -q(T - T_0)(T - T_{max})$. Function coefficients (and 95% credible intervals) fit via Bayesian inference.

Par.	Definition	Species (Sources)	Fit	Function Coefficients (95% CIs) & Optimal Temperature
a	Biting rate = 1 / gonotrophic cycle duration $(\text{day})^{-1}$	*Cx. annulirostris* (Russell 1986)	**B**	T_0 = 4.0 (0.7 – 8.5) T_{max} = 39.1 (37.9 – 40.0) $q = 1.26 \cdot 10^{-4}$ ($1.02 - 1.70 \cdot 10^{-4}$) optimum = 31.8°C
bc	Vector competence (transmission probability)	*Ae. vigilax* (Kay & Jennings 2002)	**Q**	T_0 = 6.0 (1.6 – 9.6) T_{max} = 42.7 (39.6 – 44.9) $q = 2.88 \cdot 10^{-3}$ ($2.02 - 4.27 \cdot 10^{-3}$) optimum = 24.4°C
$lf = 1/\mu$	Adult lifespan (days)	*Cx. annulirostris* (McDonald *et al.* 1980)	**Q**	T_0 = 13.0 (10.6 – 14.6) T_{max} = 33.6 (33.0 – 34.5) q = 0.241 (0.177 – 0.304) optimum = 23.4°C
PDR	Parasite development rate $(\text{day})^{-1}$	*Ae. vigilax* (Kay & Jennings 2002)	**B**	T_0 = 6.3 (1.3 – 13.0) T_{max} = 41.1 (36.1 – 45.0) $q = 1.38 \cdot 10^{-4}$ ($0.855 - 2.14 \cdot 10^{-4}$) optimum = 33.0°C
EFD	Fecundity (eggs per female per day)	*Cx. annulirostris* (McDonald *et al.* 1980)	**Q**	T_0 = 14.7 (11.9 – 17.2) T_{max} = 31.4 (30.3 – 32.9) $q = 5.84 \cdot 10^{-3}$ ($3.90 - 8.71 \cdot 10^{-3}$) optimum = 27.0°C
pRH	Raft viability (probability of raft hatching)	*Cx. annulirostris* (McDonald *et al.* 1980; Mottram *et al.* 1986)	**Q**	T_0 = 14.3 (10.6 – 17.2) T_{max} = 38.1 (33.7 – 42.0) $q = 6.78 \cdot 10^{-3}$ ($3.36 - 12.6 \cdot 10^{-3}$) optimum = 26.2°C
nLR	Within-raft egg survival (number of larvae per raft)	*Cx. annulirostris* (Mottram *et al.* 1986)	**Q**	T_0 = 17.0 (15.6 – 17.9) T_{max} = 37.2 (36.4 – 38.4) $q = 2.73 \cdot 10^{-3}$ ($1.99 - 3.29 \cdot 10^{-3}$) optimum = 27.0°C
pLA	Larval-to-adult survival (probability)	*Cx. annulirostris* (McDonald *et al.* 1980; Mottram *et al.* 1986; Rae 1990)	**Q**	T_0 = 14.9 (13.3 – 16.5) T_{max} = 39.1 (37.9 – 40.4) $q = 5.39 \cdot 10^{-3}$ ($4.31 - 6.65 \cdot 10^{-3}$) optimum = 27°C
MDR	Mosquito development rate $(\text{day})^{-1}$	*Cx. annulirostris* (McDonald *et al.* 1980; Mottram *et al.* 1986; Rae 1990)	**B**	T_0 = 11.1 (7.6 – 14.4) T_{max} = 39.2 (37.9 – 40.1) $q = 6.86 \cdot 10^{-5}$ ($5.47 - 8.47 \cdot 10^{-5}$) optimum = 32.6°C

TABLE S3: Trait thermal response functions and data sources for Murray Valley Encephalitis virus and additional vector species (*Ae. notoscriptus* and *Ae. camptorhynchus*). 'Par.' = model parameter. Results are given for fits from data-informed priors. Asymmetrical responses fit with Brière function (**B**): $B(T) = qT(T - T_0)(T_{max} - T)^{1/2}$; symmetrical responses fit with quadratic function (**Q**): $Q(T) = -q(T - T_0)(T - T_{max})$. Function coefficients (and 95% credible intervals) fit via Bayesian inference.

Par.	Definition	Species (Sources)	Fit	Function Coefficients (95% CIs) & Optimal Temperature
bc	Vector competence (transmission probability)	MVEV in *Cx. Annulirostris* (Kay *et al.* 1989)	**NA**	Did not fit because no temperature signal
PDR	Parasite development rate $(\text{day})^{-1}$	MVEV in *Cx. Annulirostris* (Kay *et al.* 1989)	**B**	T_0 = 12.8 (6.6 – 19.0) T_{max} = 41.9 (38.6 – 45.0) $q = 1.04 \cdot 10^{-4}$ ($0.641–1.55 \cdot 10^{-4}$) optimum = 34.8°C
pLA	Larval-to-adult survival (probability)	*Ae. camptorhynchus* (Barton & Aberton 2005)	**Q**	T_0 = 5.5 (1.9 – 10.1) T_{max} = 38.6 (35.7 – 42.3) $q = 3.02 \cdot 10^{-3}$ ($2.00 – 4.83 \cdot 10^{-3}$) optimum = 22.2°C
pLA	Larval-to-adult survival (probability)	*Ae. notoscriptus* (Williams & Rau 2011)	**Q**	T_0 = 9.1 (7.1 – 11.0) T_{max} = 36.2 (34.7 – 37.9) $q = 5.72 \cdot 10^{-3}$ ($4.37 – 7.32 \cdot 10^{-3}$) optimum = 22.8°C
MDR	Mosquito development rate $(\text{day})^{-1}$	*Ae. camptorhynchus* (Barton & Aberton 2005)	**B**	T_0 = 9.5 (1.8 – 19.1) T_{max} = 38.8 (37.2 – 40.3) $q = 4.57 \cdot 10^{-5}$ ($2.50 – 8.29 \cdot 10^{-5}$) optimum = 32.2°C
MDR	Mosquito development rate $(\text{day})^{-1}$	*Ae. notoscriptus* (Williams & Rau 2011)	**B**	T_0 = 9.6 (6.4 – 12.9) T_{max} = 38.7 (37.1 – 40.0) $q = 6.86 \cdot 10^{-5}$ ($5.43 – 8.56 \cdot 10^{-5}$) optimum = 32.0°C

TABLE S4: Trait thermal response functions and data sources used to parameterize priors for data-informed trait thermal responses. 'Par.' = model parameter. Fits were made with uniform priors. Asymmetrical responses fit with Brière function (**B**): $B(T) = qT(T - T_0)(T_{max} - T)^{1/2}$; symmetrical responses fit with quadratic function (**Q**): $Q(T) = -q(T - T_0)(T - T_{max})$. Function coefficients (and 95% credible intervals) fit via Bayesian inference.

Par.	Definition	Species (Sources)	Fit	Function Coefficients (95% CIs) & Optimal Temperature
a	Biting rate = 1 / gonotrophic cycle duration $(\text{day})^{-1}$	*Anopheles pseudopunctipennis* (Lardeux *et al.* 2008); *Ae. aegypti* (Focks *et al.* 1993; Focks & Barrera 2006; Morin *et al.* 2015)	**B**	T_0 = 16.5 (14.0 – 18.3) T_{max} = 39.3 (37.7 – 40.0) $q = 3.03 \cdot 10^{-4}$ ($2.35 - 3.78 \cdot 10^{-4}$) optimum = 33.6°C
bc	Vector competence (transmission probability)			Did not use priors because they were asymmetric (B) while data were symmetric (Q)
lf	Adult lifespan (days)	*Ae. aegypti* (Beserra *et al.* 2009; Yang *et al.* 2009)	**Q**	T_0 = 6.4 (1.5 – 9.9) T_{max} = 39.3 (36.6 – 43.4) q = 0.109 (0.0631 – 0.164) optimum = 23.0°C
PDR	Parasite development rate $(\text{day})^{-1}$	Dengue in *Ae. aegypti* (Davis 1932; McLean *et al.* 1974; Watts *et al.* 1987; Focks *et al.* 1993; Focks & Barrera 2006; Carrington *et al.* 2013; Tjaden *et al.* 2013); dengue in *Ae. Albopictus* (Xiao *et al.* 2014)	**B**	T_0 = 14.4 (4.1 – 19.5) T_{max} = 41.9 (38.1 – 44.9) $q = 1.05 \cdot 10^{-4}$ ($0.532 - 1.71 \cdot 10^{-4}$) optimum = 35.0°C
EFD	Fecundity (eggs per female per day)	*Ae. aegypti* (Beserra *et al.* 2009; Yang *et al.* 2009); *Ae. albopictus* (Calado & Navarro-Silva 2002); *Ae. krombeini* (Joshi 1996)	**Q**	T_0 = 13.4 (2.9 – 19.3) T_{max} = 33.9 (31.9 – 36.7) $q = 9.47 \cdot 10^{-3}$ ($3.47 - 19.0 \cdot 10^{-3}$) optimum = 28.8°C
pRH	Raft viability (probability of raft hatching)			No data for priors
nLR	Within-raft egg survival (number of larvae per raft)			No data for priors

pLA	Larval-to-adult survival (probability)	*Ae. aegypti* (Rueda *et al.* 1990; Tun-Lin *et al.* 2000; Kamimura *et al.* 2002; Westbrook *et al.* 2010; Eisen *et al.* 2014); *Ae. Albopictus* (Teng & Apperson 2000; Wiwatanaratanabutr & Kittayapong 2006; Delatte *et al.* 2009; Westbrook *et al.* 2010; Muturi *et al.* 2011); *Ae. triseriatus* (Jalil 1972)	**Q**	T_0 = 12.5 (11.2 – 13.6) T_{max} = 38.2 (37.3 – 39.2) q = 5.31 (4.41 – 6.24) optimum = 25.4 °C
MDR	Mosquito development rate $(\text{day})^{-1}$	*Ae. aegypti* (Rueda *et al.* 1990; Tun-Lin *et al.* 2000; Kamimura *et al.* 2002); *Ae. albopictus* (Yee unpublished data) (Alto & Juliano 2001; Briegel & Timmermann 2001; Calado & Navarro-Silva 2002; Wiwatanaratanabutr & Kittayapong 2006; Delatte *et al.* 2009; Westbrook *et al.* 2010; Muturi *et al.* 2011; Ezeakacha 2015); *Ae. triseriatus* (Jalil 1972)	**B**	T_0 = 9.6 (5.3 – 12.7) T_{max} = 38.9 (37.7 – 41.4) $q = 7.06 \cdot 10^{-5}$ ($4.98 – 8.99 \cdot 10^{-5}$) optimum = 32.2°C

FIGURE S1: **Thermal responses of *Cx. annulirostris* and Ross River virus (in *Ae. vigilax*) traits fit with uniform priors**. For lifespan (*lf*; B) and fecundity (*EFD*; D) points show data means and error bars indicate standard error (for display only; models were fit to raw data). Black solid lines are function means; dashed red lines are function 95% credible intervals. The thermal responses for vector competence (*bc*) and egg survival traits (*pRH* and *nLR*) fit with uniform priors are included in Fig. 2 (main text) because we did not use data-informed priors for those traits.

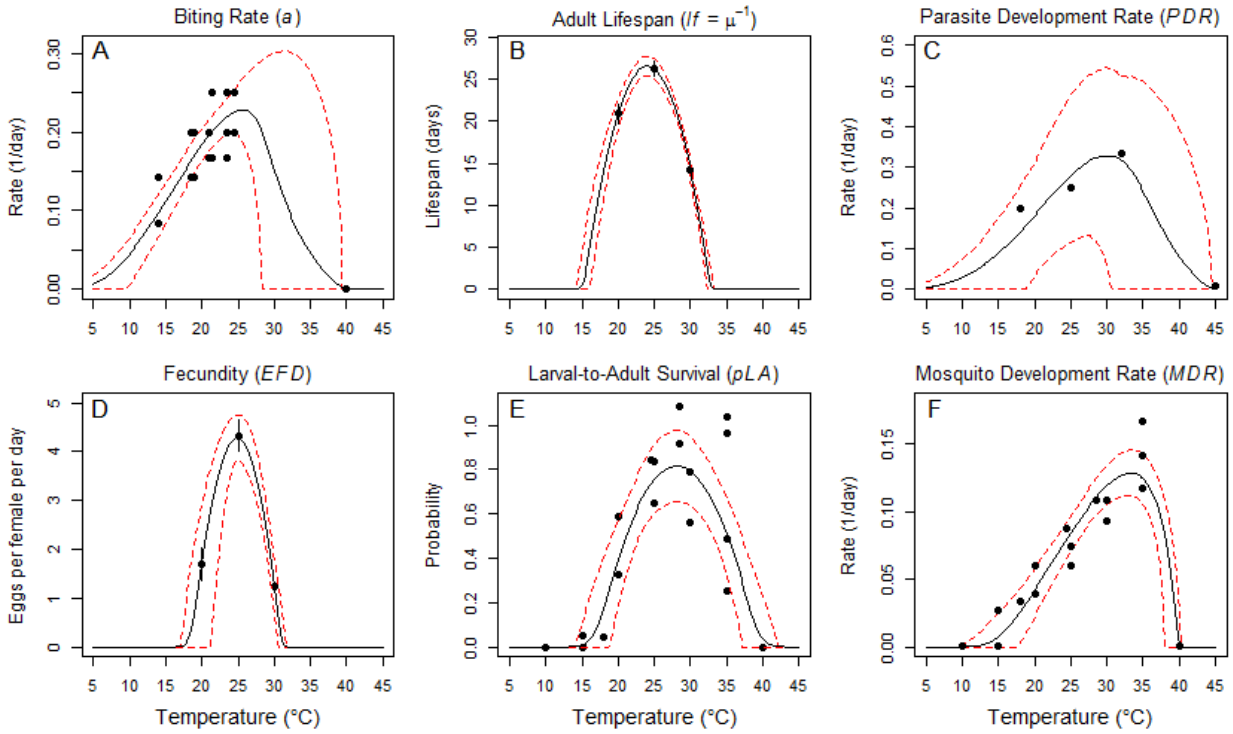

FIGURE S2: **Trait thermal responses for *Ae. camptorhynchus*.** (Top row) Mosquito development rate (*MDR*) and (bottom row) larval survival (*pLA*) fit with (left column) data-informed priors and (right column) uniform priors. Black solid lines are function means; dashed red lines are function 95% credible intervals.

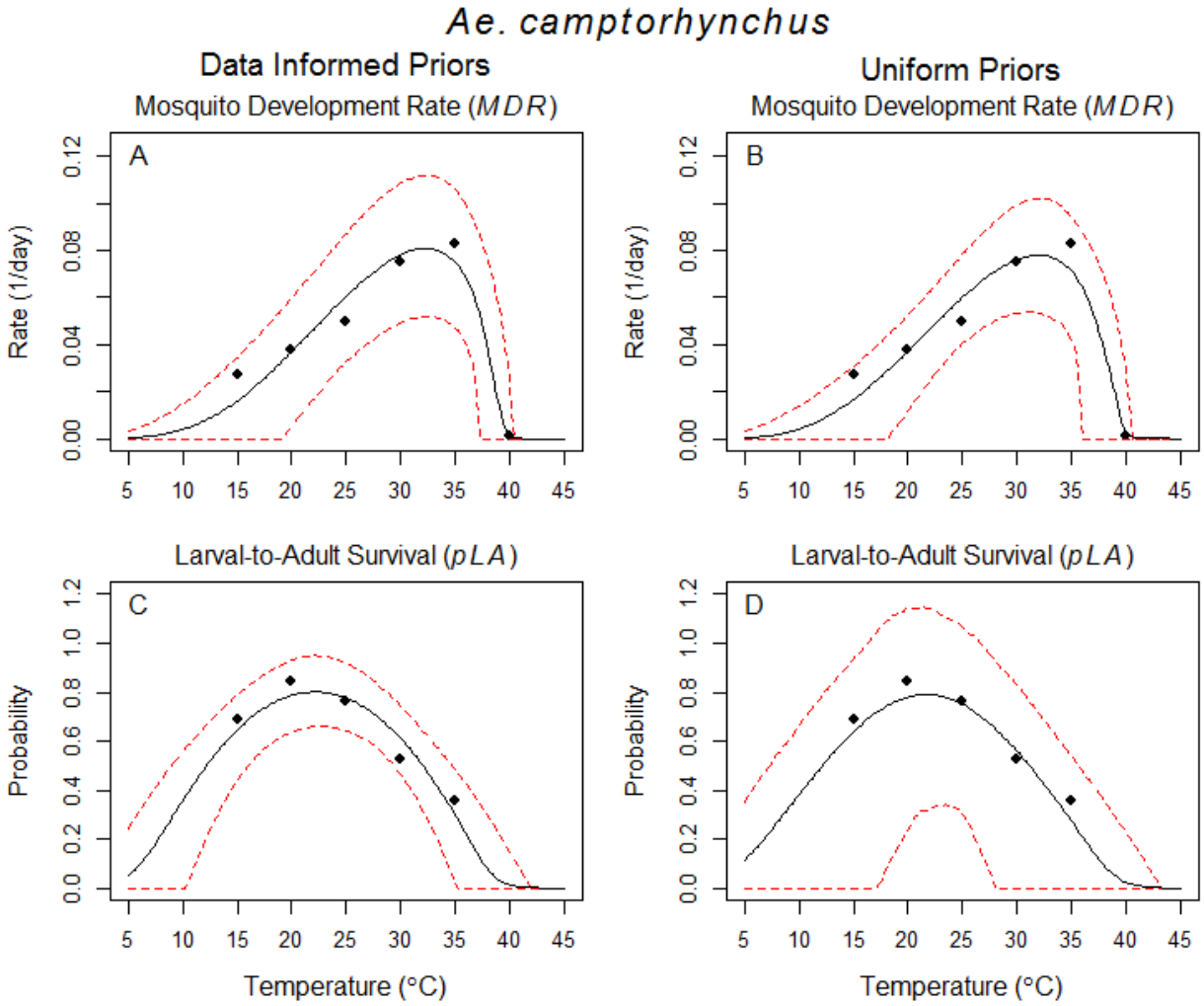

FIGURE S3: **Trait thermal responses for *Ae. notoscriptus.*** (Top row) Mosquito development rate (*MDR*) and (bottom row) larval survival (*pLA*) fit with (left column) data-informed priors and (right column) uniform priors. Black solid lines are function means; dashed red lines are function 95% credible intervals.

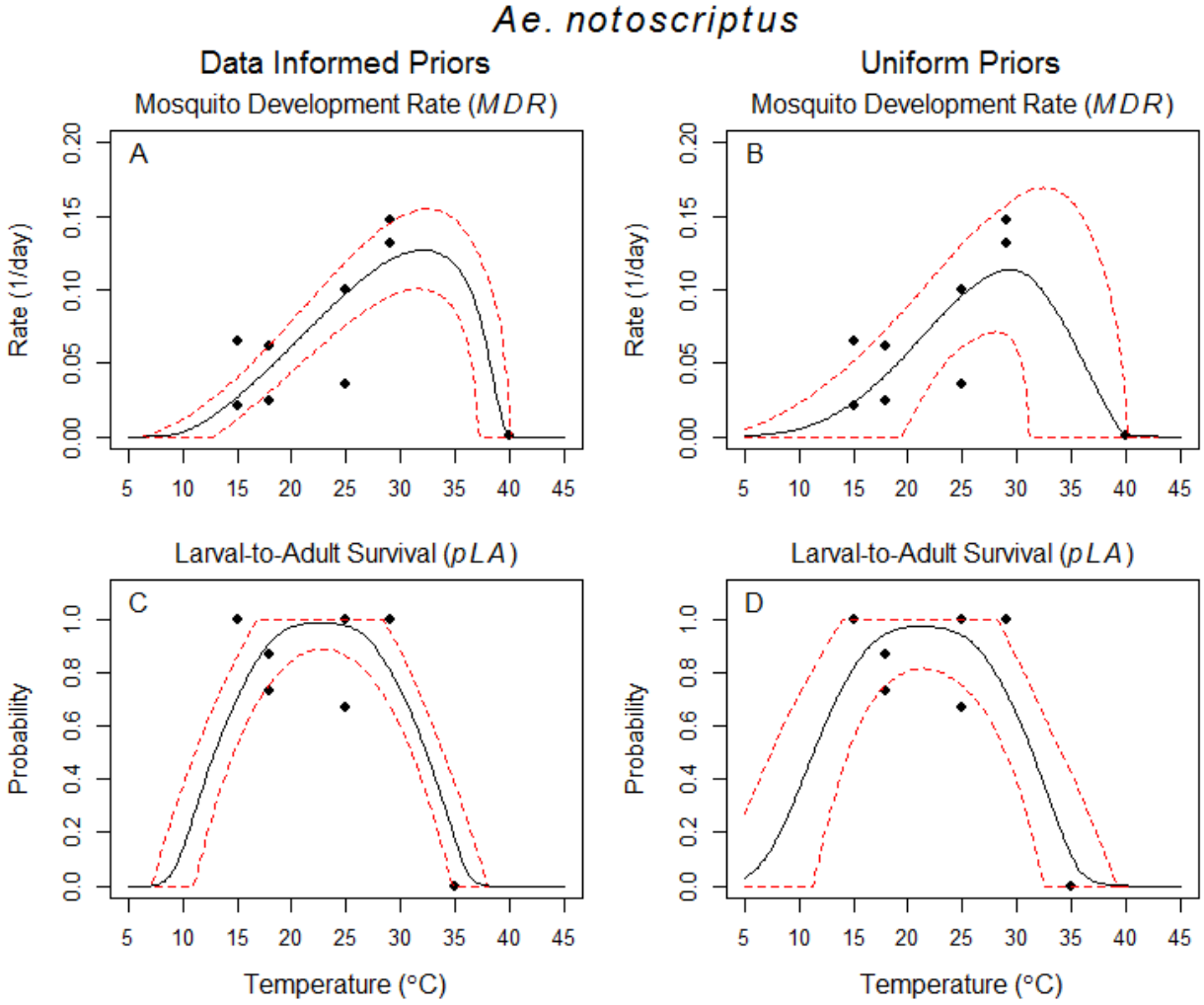

FIGURE S4: **Trait thermal responses for Murray Valley Encephalitis virus in *Cx. annulirostris***. (Top row) Pathogen development rate (*PDR*) fit with (A) data-informed priors and (B) uniform priors. Black solid lines are function means; dashed red lines are function 95% credible intervals. (C) Data for vector competence (*bc*). Gray points are temperature treatment means. Because there was no temperature signal, we did not fit a thermal response.

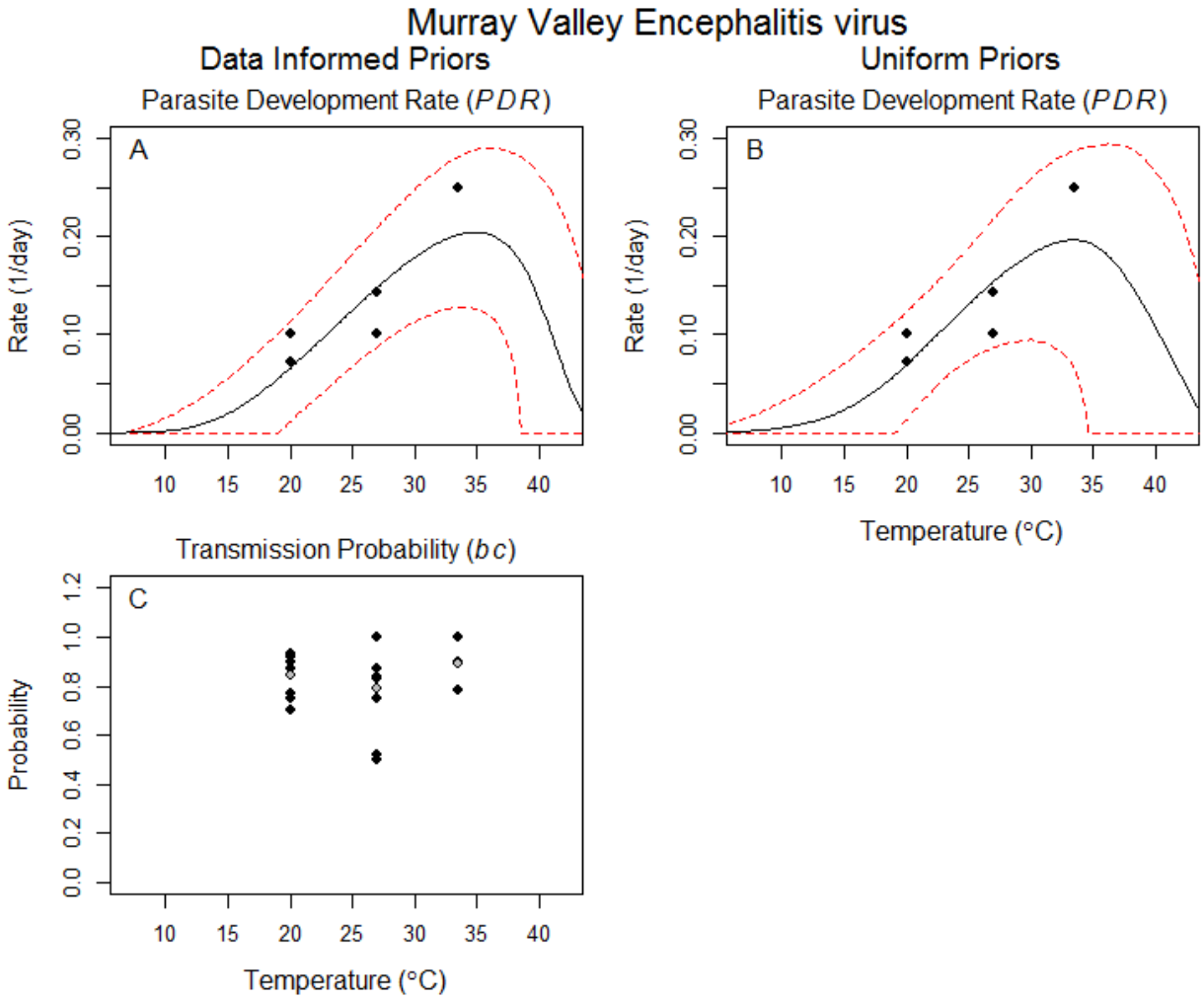

FIGURE S5: Additional R_0 and mosquito density model results. (A) R_0 (temperature-dependent *M* model, eq. 2: solid lines; constant *M* model, eq. 1: dashed lines) for Ross River virus (RRV) from traits fit with data-informed priors (black) and uniform priors (gray). (B) R_0 for RRV with partial trait data (*pLA* and *MDR*) from alternative vector species *Ae. camptorhynchus* (blue line) and *Ae. notoscriptus* (red line). Model using traits from *Cx. annulirostris* (solid black line) shown for comparison. These traits only occur in the temperature-dependent *M* model. (C) R_0 (temperature-dependent *M* model: solid lines; constant *M* model: dashed lines) for RRV (black) and Murray Valley Encephalitis virus (MVEV; purple). (D) Equilibrium mosquito density (*M*) from partial trait data (*pLA* and *MDR*) from alternative vector species *Ae. camptorhynchus* and *Ae. notoscriptus*. Lines are the same as in panel B.

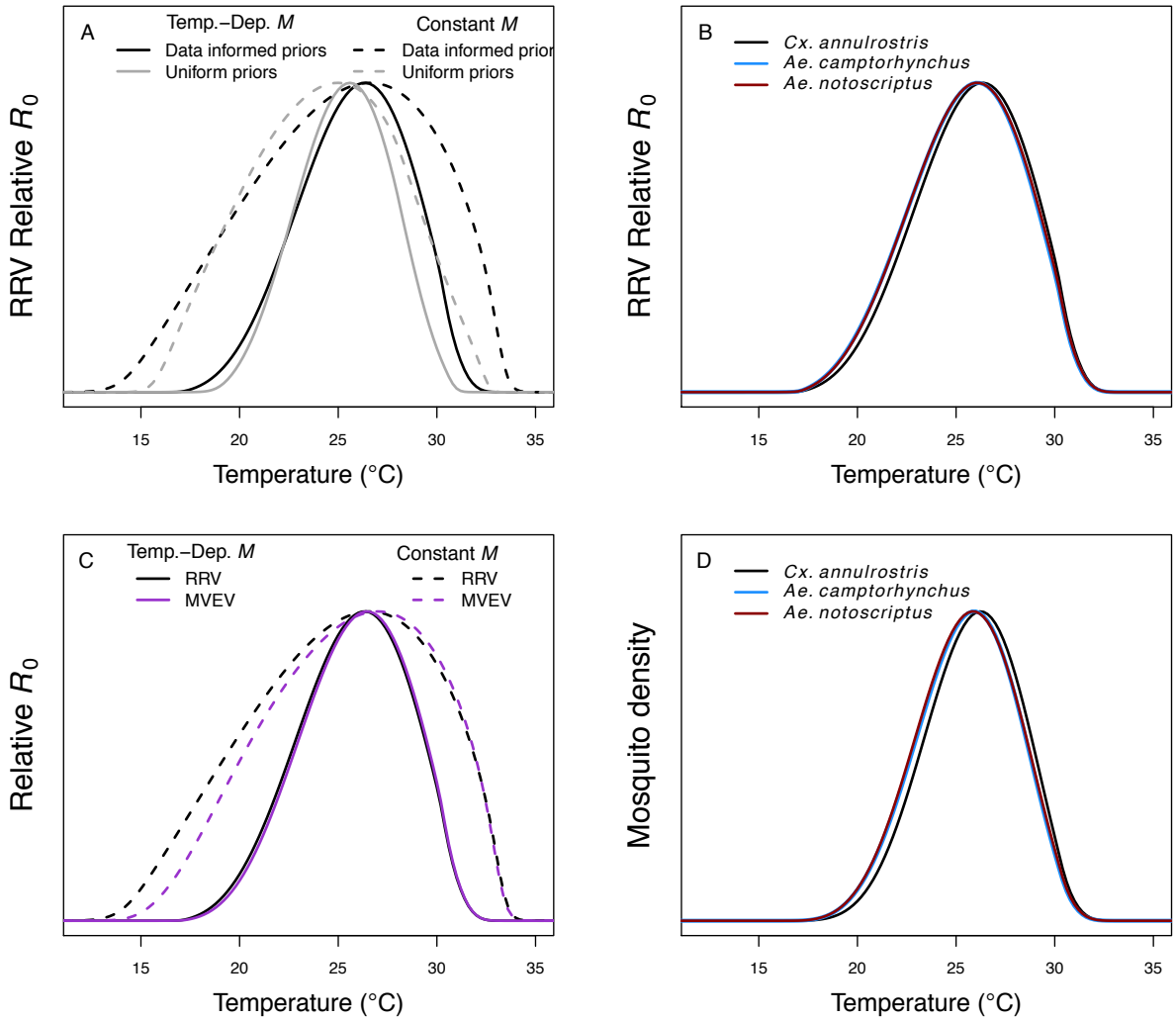

FIGURE S6: Sensitivity and uncertainty analyses of the temperature-dependent *M* model (eq. 2) to examine the effects of each trait's thermal response on the thermal response of R_0. (A) Sensitivity measured by holding one parameter constant while other parameters assume their posterior median thermal response functions. The black curve is the posterior mean of R_0. Constant parameters are: biting rate (*a*, red), vector competence (*bc*, orange), fecundity (*EFD*, tan), proportion of egg rafts hatching (*pRH*, green), number of larvae emerging per raft (*nLR*, light blue), larval-to-adult survival (*pLA*, dark blue), mosquito development rate (*MDR*, purple), lifespan ($lf = 1/\mu$, pink), and parasite development rate (*PDR*, gray). If setting a trait constant results in R_0 shifting to a higher optimum, then that trait is responsible for lowering the optimum of R_0 (and vice-versa). (B) Sensitivity measured as the partial derivatives of R_0 with respect to each trait and temperature. The thick black curve is the derivative of R_0 with respect to temperature; traits are as in panel A. (C) The relative contribution of each trait to uncertainty in R_0 across temperatures. (See Material and Methods in main text for more details.)

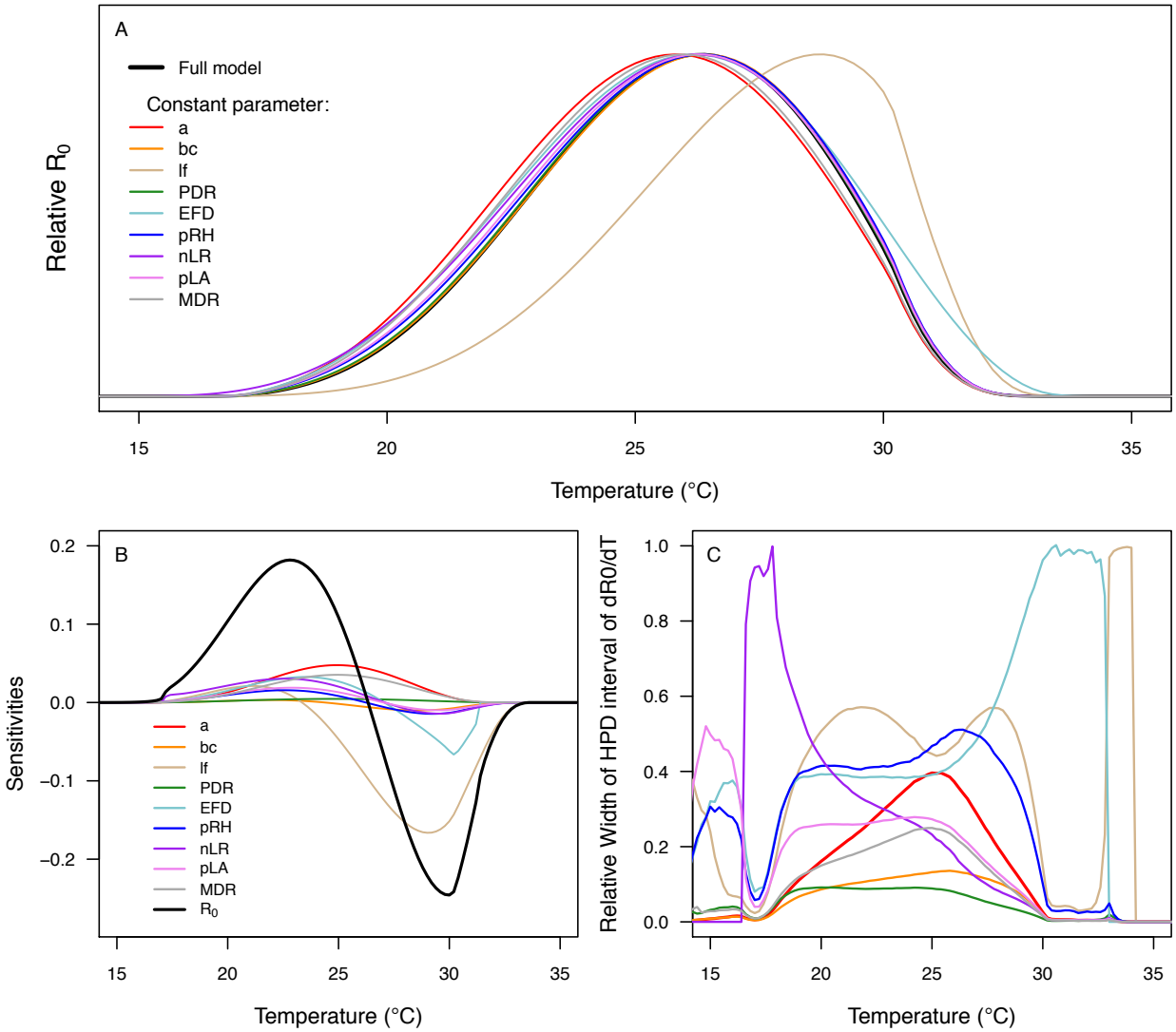

FIGURE S7: **Maps showing CIs of temperature suitability for RRV transmission.** Months where $R_0 > 0$ with (A) 2.5%, (B) 50% (median), and (C) 97.5% of the posterior probability distribution. Panel B is the same as Fig. 4A in the main text.

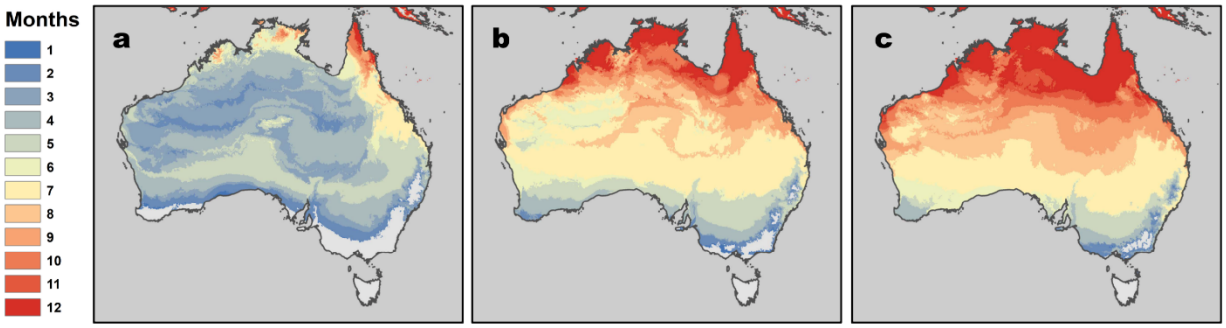

FIGURE S8: **Mean versus median RRV R_0 results.** Example showing how the upper thermal limit smoother and more visually intuitive with posterior distribution mean rather median. Throughout the main text and Appendix S1 we plot posterior distribution means but report medians of parameter values and use medians for downstream analyses (see note above).

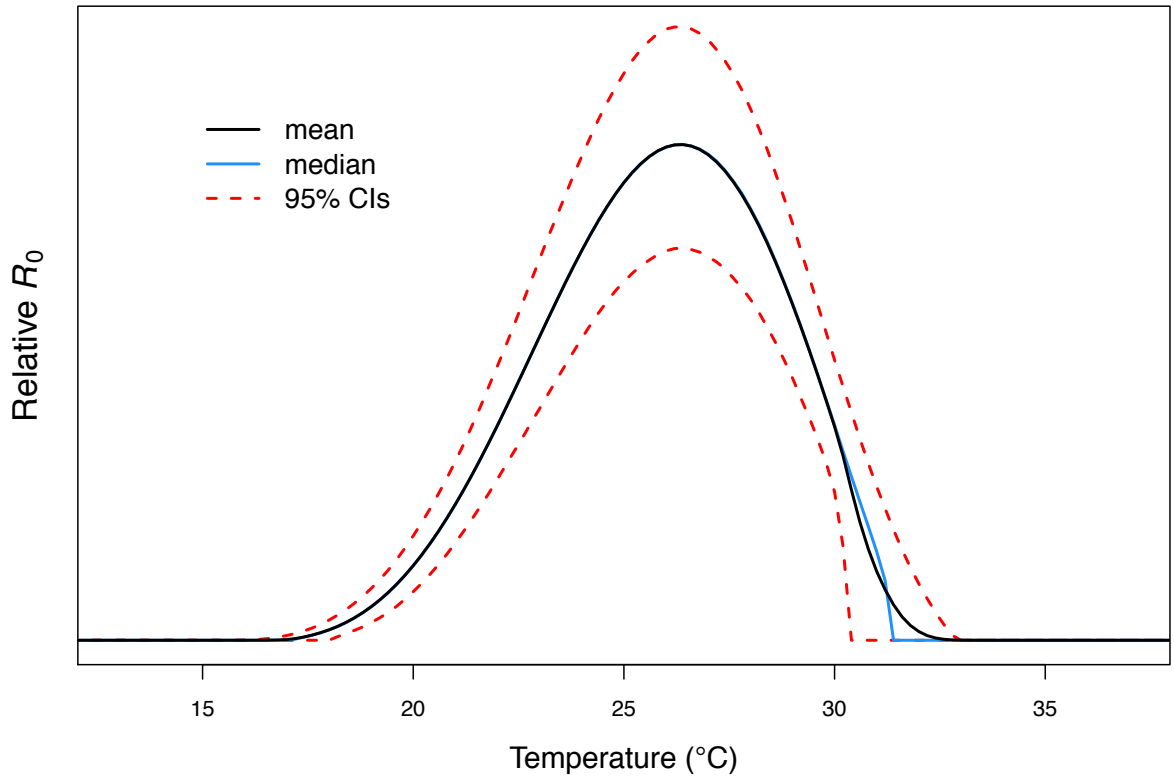

Partial Derivatives for Sensitivity Analysis

For all traits (x) that appear only in the numerator of R_0 (bc, EFD, pRH, nLR, pLA, MDR):

$$\frac{\partial R_0}{\partial x} = \frac{R_0}{2x} \qquad \text{eq. S1}$$

For biting rate (a):

$$\frac{\partial R_0}{\partial a} = \frac{R_0}{a} \qquad \text{eq. S2}$$

For parasite development rate (PDR):

$$\frac{\partial R_0}{\partial a} = \frac{R_0}{2\ lf\ PDR^2} \qquad \text{eq. S3}$$

For lifespan (lf):

$$\frac{\partial R_0}{\partial a} = \frac{R_0(1+3PDR)}{2\ PDR\ lf^2} \qquad \text{eq. S4}$$

Additional methods for survival and fecundity data from McDonald *et al.* 1980

The fecundity and adult survival data in McDonald *et al.* 1980 were both published as time series for one experimental population number over time. This approach resulted in data that needed to be formatted or transformed to better fit thermal responses via Bayesian inference.

For survival, McDonald *et al.* reported the percent surviving approximately every other day (hereafter: 'semi-daily'). We used these data——along with the number of female adults alive on the first day of oviposition at each temperature—to generate a time series estimating the number surviving on every other day. To generate the dataset that we used to directly fit the thermal responses, we converted this time series into the number of female individuals who died on each day (i.e., lifespan data).

For fecundity, McDonald *et al.* reported semi-daily fecundity data for entire population. Because the population was synchronized, and because mosquitoes lay discrete clutches of eggs separated by several days (the gonotrophic cycle duration), there were many days in the time series in which the population did not produce offspring. These zero-inflated semi-daily fecundity data are not ideal for fitting thermal responses. Therefore, after digitizing the daily fecundity time series, we binned periods of several days (the bin size varied by temperature, since the gonotrophic cycle duration varies with temperature) and took a survival-weighted average within each bin (so days with more individual mothers contributing to offspring production counted more). To generate the dataset that we used to directly fit the thermal responses, we weighted the values within each bin by the mean number of surviving mothers in that bin. This approach allowed us to remove zero points and more accurately reflect daily fecundity averaged over a non-synchronized mosquito population. NOTE: the variation captured

by these data and this approach is not variation between individual adult females, but rather variation by age for the entire population.

References

Alto, B.W. & Juliano, S.A. (2001). Temperature effects on the dynamics of *Aedes albopictus* (Diptera: Culicidae) populations in the laboratory. *J. Med. Entomol.*, 38, 548–56.

Barton, P.S. & Aberton, J.G. (2005). Larval Development and Autogeny in *Ochlerotatus camptorhynchus* (Thomson) (Diptera: Culicidae) from Southern Victoria. *Proc. Linn. Soc. New South Wales*, 126, 261–267.

Beserra, E.B., Fernandes, C.R.M., Silva, S.A. de O., Silva, L.A. da & Santos, J.W. dos. (2009). Efeitos da temperatura no ciclo de vida, exigências térmicas e estimativas do número de gerações anuais de *Aedes aegypti* (Diptera, Culicidae). *Iheringia. Série Zool.*, 99, 142–148.

Biggs, A.J.W. & Mottram, P. (2008). Links between dryland salinity, mosquito vectors, and Ross River Virus disease in southern inland Queensland—an example and potential implications. *Soil Res.*, 46, 62–66.

Briegel, H. & Timmermann, S.E. (2001). *Aedes albopictus* (Diptera: Culicidae): physiological aspects of development and reproduction. *J. Med. Entomol.*, 38, 566–71.

Brokenshire, T., Symonds, D., Reynolds, R., Doggett, S., Geary, M. & Russell, R. (2000). A cluster of locally-acquired Ross River virus infection in outer western Sydney. *NSW Public Heal. Bull*, 11, 132–134.

Calado, D.C. & Navarro-Silva, M.A. (2002). Influência da temperatura sobre a longevidade, fecundidade e atividade hematofágica de *Aedes* (Stegomyia) *albopictus* Skuse, 1894 (Diptera, Culicidae) sob condições de laboratório. *Rev. Bras. Entomol.*, 46, 93–98.

Campbell, J., Aldred, J. & Davis, G. (1989). Some aspects of the natural history of Ross River virus in south east Gippsland, Victoria. *Arbovirus Res. Aust.*, 5, 24–28.

Carrington, L.B., Armijos, M.V., Lambrechts, L. & Scott, T.W. (2013). Fluctuations at a Low Mean Temperature Accelerate Dengue Virus Transmission by *Aedes aegypti*. *PLoS Negl. Trop. Dis.*, 7, e2190.

Davis, N.C. (1932). The effect of various temperatures in modifying the extrinsic incubation periods of the yellow fever virus in *Aedes aegypti*. *Am. J. Epidemiol.*, 16, 163–176.

Delatte, H., Gimonneau, G., Triboire, A. & Fontenille, D. (2009). Influence of Temperature on Immature Development, Survival, Longevity, Fecundity, and Gonotrophic Cycles of Aedes albopictus, Vector of Chikungunya and Dengue in the Indian Ocean. *J. Med. Entomol.*, 46, 33–41.

Dhileepan, K. (1996). Mosquito seasonality and arboviral disease incidence in Murray valley, southeast Australia. *Med. Vet. Entomol.*, 10, 375–384.

Eisen, L., Monaghan, A.J., Lozano-Fuentes, S., Steinhoff, D.F., Hayden, M.H. & Bieringer, P.E. (2014). The impact of temperature on the bionomics of *Aedes* (Stegomyia) *aegypti*, with special reference to the cool geographic range margins. *J. Med. Entomol.*, 51, 496–516.

Ezeakacha, N.F. (2015). Environmental Impacts and Carry-over Effects in Complex Life Cycles: The Role of Different Life History Stages. University of Southern Mississippi.

Focks, D.A. & Barrera, R. (2006). Dengue transmission dynamics: assessment and implications for control. In: *Report of the Scientific Working Group Meeting on Dengue*. WHO, Geneva,

pp. 92–109.

Focks, D.A., Haile, D.G., Daniels, E. & Mount, G.A. (1993). Dynamic life table model for *Aedes aegypti* (Diptera: Culicidae): analysis of the literature and model development. *J. Med. Entomol.*, 30, 1003–17.

Frances, S.P., Cooper, R.D., Rowcliffe, K.L., Chen, N. & Cheng, Q. (2004). Occurrence of Ross River virus and Barmah Forest virus in mosquitoes at Shoalwater Bay military training area, Queensland, Australia. *J. Med. Entomol.*, 41, 115–20.

Harley, D., Ritchie, S., Phillips, D. & van den Hurk, A. (2000). Mosquito isolates of Ross River virus from Cairns, Queensland, Australia. *Am. J. Trop. Med. Hyg.*, 62, 561–5.

Harley, D., Sleigh, A. & Ritchie, S. (2001). Ross River Virus Transmission, Infection, and Disease: a Cross-Disciplinary Review. *Clin. Microbiol. Rev.*, 14, 909–932.

Jacups, S.P., Whelan, P.I., Markey, P.G., Cleland, S.J., Williamson, G.J. & Currie, B.J. (2008). Predictive indicators for Ross River virus infection in the Darwin area of tropical northern Australia, using long-term mosquito trapping data. *Trop. Med. Int. Heal.*, 13, 943–952.

Jalil, M. (1972). Effect of temperature on larval growth of *Aedes triseriatus*. *J. Econ. Entomol.*, 65, 625–6.

Joshi, D.S. (1996). Effect of fluctuating and constant temperatures on development, adult longevity and fecundity in the mosquito *Aedes krombeini*. *J. Therm. Biol.*, 21, 151–154.

Kamimura, K., Matsuse, I.T., Takahashi, H., Komukai, J., Fukuda, T., Suzuki, K., *et al.* (2002). Effect of temperature on the development of *Aedes aegypti* and *Aedes albopictus*. *Med. Entomol. Zool.*, 53, 53–58.

Kay, B.H., Fanning, I.D. & Mottram, P. (1989). The vector competence of *Culex annulirostris*, *Aedes sagax* and *Aedes alboannulatus* for Murray Valley encephalitis virus at different temperatures. *Med. Vet. Entomol.*, 3, 107–112.

Kay, B.H. & Jennings, C.D. (2002). Enhancement or Modulation of the Vector Competence of *Ochlerotatus vigilax* (Diptera: Culicidae) for Ross River Virus by Temperature. *J. Med. Entomol.*, 39, 99–105.

Kelly-Hope, L.A., Purdie, D.M. & Kay, B.H. (2004). Ross river virus disease in Australia, 1886-1998, with analysis of risk factors associated with outbreaks. *J. Med. Entomol.*, 41, 133–150.

Lardeux, F.J., Tejerina, R.H., Quispe, V. & Chavez, T.K. (2008). A physiological time analysis of the duration of the gonotrophic cycle of *Anopheles pseudopunctipennis* and its implications for malaria transmission in Bolivia. *Malar. J.*, 7, 141.

Lau, C., Aubry, M., Musso, D., Teissier, A., Paulous, S., Desprès, P., *et al.* (2017). New evidence for endemic circulation of Ross River virus in the Pacific Islands and the potential for emergence. *Int. J. Infect. Dis.*, 57, 73–76.

Lindsay, M., Condon, R., Mackenzie, J., Johansen, C., D'Ercole, M. & Smith, D. (1992). A major ourbreak of Ross river virus infection in the south-west of Western Australia and the Perth metropolitan area. *Comm. Dis. Int.*, 16, 290–294.

Lindsay, M., Oliveira, N., Jasinska, E., Johansen, C., Harrington, S., Wright, A.E., *et al.* (1996).

An outbreak of Ross River virus disease in Southwestern Australia. *Emerg. Infect. Dis.*, 2, 117–120.

Lindsay, M.D.A., Broom, A.K., Wright, A.E. (Tony), Johansen, C.A. & Mackenzie, J.S. (1993a). Ross River Virus Isolations from Mosquitoes in Arid Regions of Western Australia: Implication of Vertical Transmission as a Means of Persistence of the Virus. *Am. J. Trop. Med. Hyg.*, 49, 686–696.

Lindsay, M.D.A., Jardine, A., Johansen, C.A., Wright, A.E., Harrington, S.A. & Weinstein, P. (2007). Mosquito (Diptera: Culicidae) fauna in inland areas of south-west Western Australia. *Aust. J. Entomol.*, 46, 60–64.

Lindsay, M.D., Johansen, C., Broom, A.K., D'Ercole, M., Wright, A.E., Condon, R., *et al.* (1993b). The epidemiology of outbreaks of Ross River virus infection in Western Australia in 1991–1992. *Arbovirus Res. Aust.*, 6, 72–76.

McDonald, G., McLaren, I.W., Shelden, G.P. & Smith, I.R. (1980). The effect of temperature on the population growth potential of *Culex annulirostris* Skuse (Diptera: Culicidae). *Aust. J. Ecol.*, 5, 379–384.

McDonnell, L., Kolbe, T., Carvan, T. & Gilchrist, K. (1994). Outbreak of Ross River virus disease in the south west districts of NSW, summer 1993. *New South Wales Public Heal. Bull.*, 5, 98–9.

McLean, D.M., Clarke, A.M., Coleman, J.C., Montalbetti, C.A., Skidmore, A.G., Walters, T.E., *et al.* (1974). Vector capability of *Aedes aegypti* mosquitoes for California encephalitis and dengue viruses at various temperatures. *Can. J. Microbiol.*, 20, 255–62.

McManus, T.J., Russell, R.C., Wells, P.J., Clanc, J.G., Fennell, M. & Cloonan, M.J. (1992). Further studies on the epidemiology and effects of Ross River virus in Tasmania. *Arbovirus Res. Aust.*, 6, 68–72.

Merianos, A., Farland, A.M., Patel, M., Currie, B., Whelan, P., Dentith, H., *et al.* (1992). A concurrent outbreak of Barmah Forest and Ross River virus disease in Nhulunbuy, Northern Territory. *Commun. Dis. Intell.*, 16, 110–111.

Morin, C.W., Monaghan, A.J., Hayden, M.H., Barrera, R. & Ernst, K. (2015). Meteorologically Driven Simulations of Dengue Epidemics in San Juan, PR. *PLoS Negl. Trop. Dis.*, 9, e0004002.

Mottram, P., Kay, B.H. & Kettle, D.S. (1986). The effect of temperature on eggs and immature Stages of *Culex annulirostris* Skuse (Diptera: Culicidae). *Aust. J. Entomol.*, 25, 131–136.

Muturi, E.J., Lampman, R., Costanzo, K. & Alto, B.W. (2011). Effect of temperature and insecticide stress on life-history traits of *Culex restuans* and *Aedes albopictus* (Diptera: Culicidae). *J. Med. Entomol.*, 48, 243–50.

Rae, D.J. (1990). Survival and development of the immature stages of *Culex annulirostris* (Diptera: Culicidae) at the Ross River Dam in tropical eastern Australia. *J Med Entomol*, 27, 756–762.

Ritchie, S.A., Fanning, I.D., Phillips, D.A., Standfast, H.A., Mcginn, D. & Kay, B.H. (1997). Ross River Virus in Mosquitoes (Diptera: Culicidae) During the 1994 Epidemic Around Brisbane, Australia. *J. Med. Entomol.*, 34, 156–159.

Rosen, L., Gubler, D.J. & Bennett, P.H. (1981). Epidemic Polyarthritis (Ross River) Virus Infection in the Cook Islands. *Am. J. Trop. Med. Hyg.*, 30, 1294–1302.

Rueda, L.M., Patel, K.J., Axtell, R.C. & Stinner, R.E. (1990). Temperature-dependent development and survival rates of *Culex quinquefasciatus* and *Aedes aegypti* (Diptera: Culicidae). *J. Med. Entomol.*, 27, 892–8.

Russell, R.C. (1986). *Culex Annulirostris* Skuse (Diptera: Culicidae) at Appin, N.S.W.—bionomics and behavior. *Aust. J. Entomol.*, 25, 103–109.

Russell, R.C. (1994). Ross River virus: disease trends and vector ecology in Australia. *Bull. Soc. Vector Ecol.*, 19, 73–81.

Russell, R.C. (2002). Ross River Virus: Ecology and Distribution. *Ann. Rev. Entomol.*, 47, 1–31.

Russell, R.C., Cloonan, M.J., Wells, P.J. & Vale, T.G. (1991). Mosquito (Diptera: Culicidae) and Arbo virus Activity on the South Coast of New South Wales, Australia, in 1985–1988. *J. Med. Entomol.*, 28, 796–804.

Ryan, P.A., Do, K.-A. & Kay, B.H. (2000). Definition of Ross River Virus Vectors at Maroochy Shire, Australia. *J. Med. Entomol.*, 37, 146–152.

Schmaedick, M.A., Ball, T.S., Burkot, T.R. & Gurr, N.E. (2008). Evaluation of Three Traps for Sampling *Aedes polynesiensis* and Other Mosquito Species in American Samoa 1. *J. Am. Mosq. Control Assoc.*, 24, 319–322.

Teng, H.J. & Apperson, C.S. (2000). Development and survival of immature *Aedes albopictus* and *Aedes triseriatus* (Diptera: Culicidae) in the laboratory: effects of density, food, and competition on response to temperature. *J. Med. Entomol.*, 37, 40–52.

Tjaden, N.B., Thomas, S.M., Fischer, D. & Beierkuhnlein, C. (2013). Extrinsic Incubation Period of Dengue: Knowledge, Backlog, and Applications of Temperature Dependence. *PLoS Negl. Trop. Dis.*, 7, e2207.

Tun-Lin, W., Burkot, T.R. & Kay, B.H. (2000). Effects of temperature and larval diet on development rates and survival of the dengue vector *Aedes aegypti* in north Queensland, Australia. *Med. Vet. Entomol.*, 14, 31–7.

Watts, D.M., Burke, D.S., Harrison, B.A., Whitmire, R.E. & Nisalak, A. (1987). Effect of temperature on the vector efficiency of *Aedes aegypti* for dengue 2 virus. *Am. J. Trop. Med. Hyg.*, 36, 143–52.

Westbrook, C.J., Reiskind, M.H., Pesko, K.N., Greene, K.E. & Lounibos, L.P. (2010). Larval Environmental Temperature and the Susceptibility of *Aedes albopictus* Skuse (Diptera: Culicidae) to Chikungunya Virus. *Vector-Borne Zoonotic Dis.*, 10, 241–247.

Whelan, P.I., Krause, V., Horsburgh, K., Sutherland, G. & Rossiter, J. (1995). Confirmed case of Ross River virus infection acquired in Alice Springs March 1995. *North. Territ. Commun. Dis. Bull.*, 2, 9–11.

Whelan, P.I., Merianos, A., Hayes, G. & Krause, V. (1997). Ross River Virus Transmission in Darwin, Northern Territory, Australia. *Arbovirus Res. Aust.*, 7, 337–345.

Whelan, P.I., Merianos, A., Patel, M.S., Tai, K.S. & Currie, B. (1992). The epidemiology of arbovirus infection in the Northern Territory 1980-92. *Arbovirus Res. Aust.*, 6, 266–70.

Wilkerson, R.C., Linton, Y.-M., Fonseca, D.M., Schultz, T.R., Price, D.C. & Strickman, D.A. (2015). Making Mosquito Taxonomy Useful: A Stable Classification of Tribe Aedini that Balances Utility with Current Knowledge of Evolutionary Relationships. *PLoS One*, 10, e0133602.

Williams, C.R. & Rau, G. (2011). Growth and development performance of the ubiquitous urban mosquito *Aedes notoscriptus* (Diptera: Culicidae) in Australia varies with water type and temperature. *Aust. J. Entomol.*, 50, 195–199.

Wiwatanaratanabutr, S. & Kittayapong, P. (2006). Effects of temephos and temperature on Wolbachia load and life history traits of *Aedes albopictus*. *Med. Vet. Entomol.*, 20, 300–7.

Xiao, F.-Z., Zhang, Y., Deng, Y.-Q., He, S., Xie, H.-G., Zhou, X.-N., *et al.* (2014). The effect of temperature on the extrinsic incubation period and infection rate of dengue virus serotype 2 infection in *Aedes albopictus*. *Arch. Virol.*, 159, 3053–3057.

Yang, H.M., Macoris, M.L.G., Galvani, K.C., Andrighetti, M.T.M. & Wanderley, D.M. V. (2009). Assessing the effects of temperature on the population of *Aedes aegypti*, the vector of dengue. *Epidemiol. Infect.*, 137, 1188–202.